

## Design, synthesis and biological evaluation of a new series of carvedilol derivatives that protect sensory hair cells from aminoglycoside-induced damage by blocking the mechanoelectrical transducer channel

Article (Accepted Version)

O'Reilly, Molly, Kirkwood, Nerissa K, Kenyon, Emma J, Huckvale, Rosemary, Cantillon, Daire M, Waddell, Simon J, Ward, Simon E, Richardson, Guy P, Kros, Corné J and Derudas, Marco (2019) Design, synthesis and biological evaluation of a new series of carvedilol derivatives that protect sensory hair cells from aminoglycoside-induced damage by blocking the mechanoelectrical transducer channel. *Journal of Medicinal Chemistry*, 62 (11). pp. 5312-5329. ISSN 0022-2623

This version is available from Sussex Research Online: <http://sro.sussex.ac.uk/id/eprint/83857/>

This document is made available in accordance with publisher policies and may differ from the published version or from the version of record. If you wish to cite this item you are advised to consult the publisher's version. Please see the URL above for details on accessing the published version.

### **Copyright and reuse:**

Sussex Research Online is a digital repository of the research output of the University.

Copyright and all moral rights to the version of the paper presented here belong to the individual author(s) and/or other copyright owners. To the extent reasonable and practicable, the material made available in SRO has been checked for eligibility before being made available.

Copies of full text items generally can be reproduced, displayed or performed and given to third parties in any format or medium for personal research or study, educational, or not-for-profit purposes without prior permission or charge, provided that the authors, title and full bibliographic details are credited, a hyperlink and/or URL is given for the original metadata page and the content is not changed in any way.

Article

## Design, synthesis and biological evaluation of a new series of carvedilol derivatives that protect sensory hair cells from aminoglycoside-induced damage by blocking the mechano-electrical transducer channel

Molly O'Reilly, Nerissa K Kirkwood, Emma J Kenyon, Rosemary Huckvale, Daire M Cantillon, Simon J Waddell, Simon E Ward, Guy P Richardson, Corne J. Kros, and Marco Derudas

*J. Med. Chem.*, **Just Accepted Manuscript** • DOI: 10.1021/acs.jmedchem.8b01325 • Publication Date (Web): 14 May 2019

Downloaded from <http://pubs.acs.org> on May 20, 2019

### Just Accepted

"Just Accepted" manuscripts have been peer-reviewed and accepted for publication. They are posted online prior to technical editing, formatting for publication and author proofing. The American Chemical Society provides "Just Accepted" as a service to the research community to expedite the dissemination of scientific material as soon as possible after acceptance. "Just Accepted" manuscripts appear in full in PDF format accompanied by an HTML abstract. "Just Accepted" manuscripts have been fully peer reviewed, but should not be considered the official version of record. They are citable by the Digital Object Identifier (DOI®). "Just Accepted" is an optional service offered to authors. Therefore, the "Just Accepted" Web site may not include all articles that will be published in the journal. After a manuscript is technically edited and formatted, it will be removed from the "Just Accepted" Web site and published as an ASAP article. Note that technical editing may introduce minor changes to the manuscript text and/or graphics which could affect content, and all legal disclaimers and ethical guidelines that apply to the journal pertain. ACS cannot be held responsible for errors or consequences arising from the use of information contained in these "Just Accepted" manuscripts.



ACS Publications

is published by the American Chemical Society, 1155 Sixteenth Street N.W., Washington, DC 20036

Published by American Chemical Society. Copyright © American Chemical Society. However, no copyright claim is made to original U.S. Government works, or works produced by employees of any Commonwealth realm Crown government in the course of their duties.

**Design, synthesis and biological evaluation of a new series of carvedilol derivatives that protect sensory hair cells from aminoglycoside-induced damage by blocking the mechano-electrical transducer channel**

**Molly O'Reilly<sup>†||</sup>, Nerissa K. Kirkwood<sup>†||</sup>, Emma J. Kenyon<sup>†</sup>, Rosemary Huckvale<sup>‡</sup>, Daire M. Cantillon<sup>⊥</sup>, Simon J. Waddell<sup>⊥</sup>, Simon E. Ward<sup>‡§</sup>, Guy P. Richardson<sup>†</sup>, Corné J. Kros<sup>†</sup> and Marco Derudas<sup>‡\*</sup>**

<sup>†</sup>Sussex Neuroscience, School of Life Sciences, University of Sussex, Falmer, Brighton, BN1 9QJ, UK

<sup>‡</sup>Sussex Drug Discovery Centre, School of Life Sciences, University of Sussex, Falmer, Brighton, BN1 9QJ, UK

<sup>⊥</sup>Wellcome Trust Centre for Global Health Research, Brighton and Sussex Medical School, University of Sussex, Falmer, Brighton, BN1 9PX, UK

<sup>§</sup>Medicines Discovery Institute, Cardiff University, Park Place, Cardiff, CF10 3AT, United Kingdom

\* Email: [m.derudas@sussex.ac.uk](mailto:m.derudas@sussex.ac.uk); Phone +44(0)1273876591

**Abstract:**

Aminoglycosides (AGs) are broad-spectrum antibiotics used for the treatment of serious bacterial infections but have use-limiting side effects including irreversible hearing loss. Here, we assessed the otoprotective profile of carvedilol in mouse cochlear cultures and *in vivo* zebrafish assays and investigated its mechanism of protection which we found may be mediated by block of the hair cell's mechano-electrical transducer (MET) channel, the major entry route for the AGs. To understand the full otoprotective potential of carvedilol, a series of 18 analogues were prepared and evaluated for their effect against AG-induced damage as well as their affinity for the MET channel. One derivative was found to confer greater protection than carvedilol itself in cochlear cultures, and also to bind more tightly to the MET channel. At higher concentrations both carvedilol and this derivative were toxic in cochlear cultures but not in zebrafish, suggesting a good therapeutic window under *in vivo* conditions.

1  
2  
3  
4  
5  
6  
7  
8  
9  
10  
11  
12  
13  
14  
15  
16  
17  
18  
19  
20  
21  
22  
23  
24  
25  
26  
27  
28  
29  
30  
31  
32  
33  
34  
35  
36  
37  
38  
39  
40  
41  
42  
43  
44  
45  
46  
47  
48  
49  
50  
51  
52  
53  
54  
55  
56  
57  
58  
59  
60

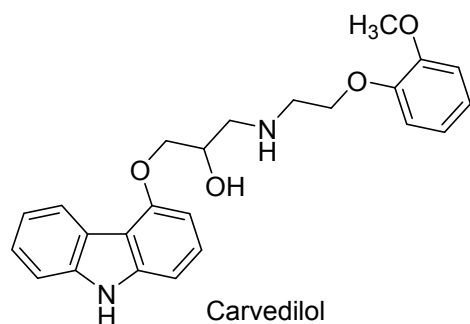
1  
2  
3  
4  
5  
6  
7  
8  
9  
10  
11  
12  
13  
14  
15  
16  
17  
18  
19  
20  
21  
22  
23  
24  
25  
26  
27  
28  
29  
30  
31  
32  
33  
34  
35  
36  
37  
38  
39  
40  
41  
42  
43  
44  
45  
46  
47  
48  
49  
50  
51  
52  
53  
54  
55  
56  
57  
58  
59  
60

**Introduction:**

AGs are broad-spectrum antibiotics widely prescribed to treat severe bacterial infections.<sup>1-3</sup> Despite being highly efficacious, they cause unfortunate side effects such as reversible nephrotoxicity and irreversible hearing loss, with the latter occurring in up to 25% of treated patients.<sup>4</sup> The AGs can enter the sensory hair cells of the inner ear through both endocytic processes<sup>5</sup> and specialised cation channels, the MET channels that are located at the tips of the stereocilia and are responsible for the detection of sounds and body movements.<sup>6-9</sup> The mechanism of ototoxicity is not fully understood and it differs amongst the various AGs, with neomycin and gentamicin for instance being shown to activate different cell-death pathways once inside zebrafish lateral line hair cells.<sup>10-12</sup> Once inside the cell they are thought to interact with various targets such as ribosomes, the endoplasmic reticulum and mitochondria<sup>13, 14</sup> leading to the production of cytotoxic levels of reactive oxygen species (ROS) which, in turn, cause apoptosis.<sup>15</sup> It is this AG-induced hair cell death that underlies the hearing loss associated with clinical drug treatments. Aside from the redesign of novel AGs<sup>16, 17</sup> or hair cell regeneration approaches,<sup>18</sup> methods aimed at preventing this use-limiting side effect have primarily focussed on either preventing the entry of AGs into hair cells by identifying blockers of the MET channel<sup>14</sup> or by reducing the cellular accumulation of ROS, often by application of antioxidants, in an attempt to prevent the induction of apoptosis.<sup>14, 19</sup> Recent efforts in this field have led to the

1 identification of otoprotective agents able to reduce or prevent the AG-induced hearing loss both  
2 in *in vitro*<sup>20-23</sup> and in *in-vivo* models of AG ototoxicity.<sup>24</sup>

3 Here we investigated the otoprotective potential of carvedilol, an FDA-approved non-selective  
4  $\alpha$ 1- and  $\beta$ -adrenergic blocker (Figure 1), used clinically for the treatment of hypertension, angina  
5 and symptomatic chronic heart failure. Carvedilol has previously been reported to protect against  
6 neomycin damage in lateral line hair cells of zebrafish when tested at 10  $\mu$ M against 200  $\mu$ M  
7 neomycin.<sup>22</sup> In addition, carvedilol did not abrogate the antimicrobial properties of neomycin,  
8 making any interference with the bactericidal activity of AGs unlikely<sup>22</sup> and making it an ideal  
9 chemical starting point for further investigation.



11 Figure 1: structure of carvedilol, a non-selective  $\alpha$ 1- and  $\beta$ -adrenergic blocker.

12 In this study, we report its protective properties against gentamicin-induced hair cell damage in  
13 mouse cochlear cultures. We propose the mechanism by which it offers otoprotection with data  
14 supporting the block of the MET channel as being responsible for its otoprotective effect. We  
15 synthesised and evaluated a series of novel carvedilol derivatives aimed at improving the  
16 protective efficacy and affinity for the MET channel, whilst concurrently reducing toxicity as  
17 well as this compound as chemical starting point for future drug development

## 18 Results

## 1 Carvedilol protects mammalian sensory hair cells from gentamicin damage

2 Mouse cochlear cultures were used to assess whether carvedilol can protect mammalian hair  
3 cells from the death induced by exposure to 5  $\mu$ M gentamicin for 48 h. A concentration of 5  $\mu$ M  
4 gentamicin is optimal, as it is close to the estimated concentration of 1  $\mu$ M gentamicin reached in  
5 the endolymph *in vivo* at the onset of ototoxic symptoms<sup>25</sup> and it kills >90% of the basal cells  
6 while sparing the apical cells, consistent with the predominantly high-frequency hearing loss  
7 observed in patients treated with aminoglycosides.<sup>4</sup> On average, incubation with 5  $\mu$ M  
8 gentamicin caused a loss of 86% of outer hair cells (OHCs) from the mid-basal region of the  
9 cochlea, with  $110 \pm 2.2$  ( $n = 26$ ) OHCs present in a 300  $\mu$ m long segment of the control and only  
10  $15 \pm 2.2$  ( $n = 26$ ) in the gentamicin-treated culture ( $p < 0.001$ ) (Figure 2A, B). Subsequently,  
11 mouse cochlear cultures were co-incubated with 5  $\mu$ M gentamicin together with escalating  
12 concentrations of carvedilol with the aim to identify the minimal concentration required to  
13 provide full protection. When tested at 5  $\mu$ M, carvedilol provided partial protection, with OHC  
14 survival differing significantly from that in both the control and gentamicin-only treated cultures  
15 ( $p < 0.001$  in both cases), suggesting that this concentration is at the limit of its protective  
16 efficacy (Figure 2C). When tested at 10  $\mu$ M and 20  $\mu$ M carvedilol provided complete protection  
17 against the gentamicin-induced loss of OHCs ( $p < 0.001$ ) (Figure 2D, E respectively). Higher  
18 concentrations of carvedilol ( $\geq 30$   $\mu$ M) proved to be generally cytotoxic, with widespread cell  
19 death observed (Figure 2F).

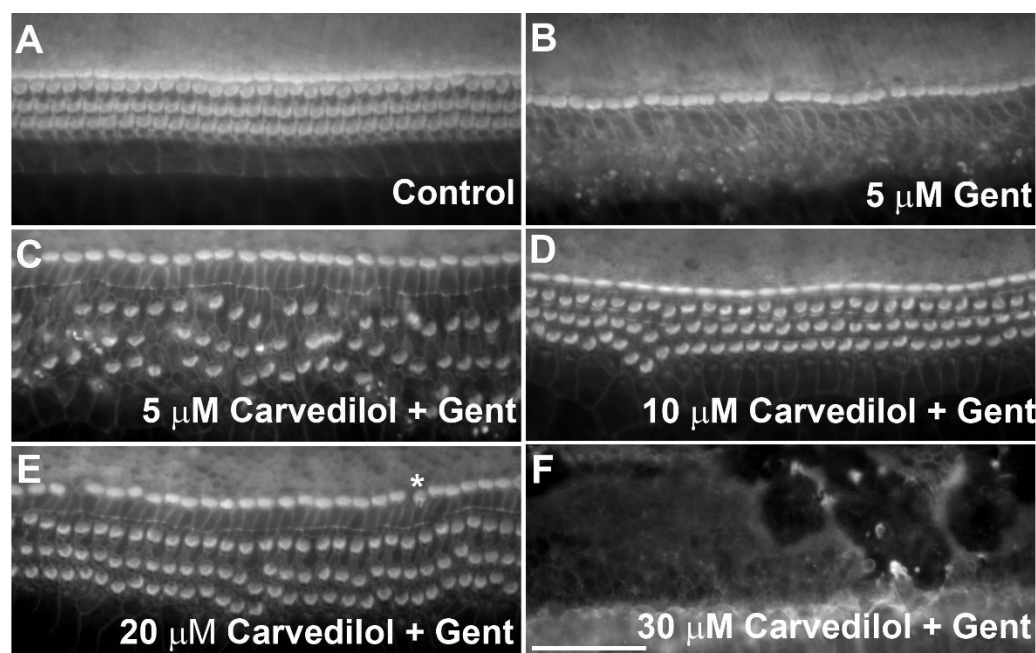


**Figure 2.** Protective effect of carvedilol against gentamicin-induced damage in a mouse cochlear culture assay. Control cultures exposed to either 0.5% DMSO (A) or 5  $\mu$ M gentamicin + 0.5% DMSO (B) for 48 h. When co-incubated with 5  $\mu$ M gentamicin, carvedilol was found to be partially protective at 5  $\mu$ M (C), fully protective at 10 and 20  $\mu$ M (D and E respectively) and generally cytotoxic at  $\geq 30$   $\mu$ M (F). The asterisk in (E) indicates an example of IHC hair bundle disruption. Scale bar is 50  $\mu$ m.

When carvedilol was tested alone no OHC death was observed at either 10  $\mu$ M or 20  $\mu$ M, with hair cell numbers similar to those observed in controls (Figure 3 A-D). Some degree of inner hair cell (IHC) damage and disruption to hair bundle morphology in both IHCs and OHCs can be observed when tested at 20  $\mu$ M both alone and in combination with 5  $\mu$ M gentamicin (Figure 2E, Figure 3D). Figures 3E and F show confocal images of IHC stereociliary bundles in control



1  
2  
3  
4  
5  
6  
7  
8  
9  
10  
11  
12  
13  
14  
15  
16  
17  
18  
19  
20  
21  
22  
23  
24  
25  
26  
27  
28  
29  
30  
31  
32  
33  
34  
35  
36  
37  
38  
39  
40  
41  
42  
43  
44  
45  
46  
47  
48  
49  
50  
51  
52  
53  
54  
55  
56  
57  
58  
59  
60

1 conditions (Figure 3E) and after exposure to 20  $\mu$ M carvedilol (Figure 3F), revealing the full  
2 extent of morphological disruption caused by carvedilol.

3 At concentrations  $\geq 30$   $\mu$ M, carvedilol is generally cytotoxic to all cell types in cochlear cultures,  
4 both alone and in the presence of 5  $\mu$ M gentamicin (Figure 2F, Figure 3G, H). Figure 3I  
5 summarises the quantification of OHC survival through analysis of the mid-basal region of  
6 cochlear cultures for both carvedilol alone and also co-exposed with gentamicin.

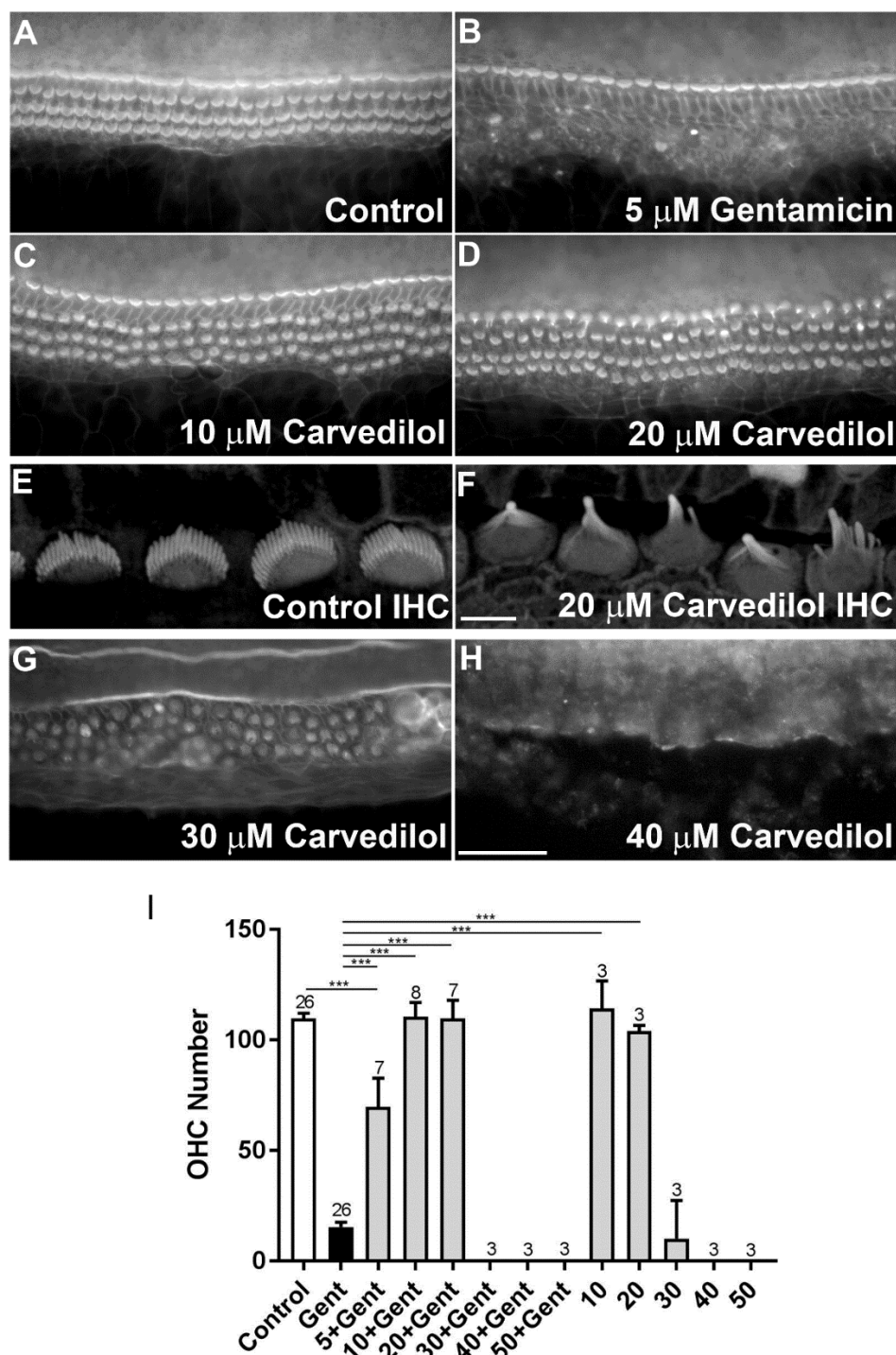


**Figure 3.** Carvedilol disrupts mechanosensory hair bundles at 20  $\mu\text{M}$ , and generally cytotoxic *in vitro* at  $\geq 30$   $\mu\text{M}$ . Cochlear cultures were exposed for 48 h to 0.5% DMSO (A and E), 5  $\mu\text{M}$  gentamicin + 0.5% DMSO (B), and escalating concentrations of carvedilol: 10  $\mu\text{M}$  (C), 20  $\mu\text{M}$

(D and F), 30  $\mu$ M (G) and 40  $\mu$ M (H). Scale bar is 10  $\mu$ m (F) and 50  $\mu$ m (H). Quantification of hair cell survival in a 300  $\mu$ m long segment of the mid-basal region of cochlear cultures is reported in I.

**Carvedilol exerts its otoprotective effect by acting as a permeant blocker of the hair cell's MET channel**

Despite a narrow therapeutic window *in vitro*, we decided to investigate the potential mechanism by which carvedilol provides its protective effect. It is well established that AGs can enter hair cells via their MET channels<sup>7,9</sup> and that block of this channel reduces or prevents their entry into the cells, thereby protecting them from any toxicity resulting from intracellular accumulation. To determine whether carvedilol protects via an interaction with the MET channel, we recorded MET currents from OHCs both before and during extracellular superfusion of carvedilol at concentrations of 1, 3 and 10  $\mu$ M.

Figure 4A shows an example of the MET currents recorded before (black), during (red) and after (blue) exposure to carvedilol (10  $\mu$ M), at membrane potentials ranging from -164 mV to +96 mV. Carvedilol reduces the size of MET currents at all membrane potentials, with this reduction particularly pronounced at intermediate and depolarized potentials. Upon re-exposure to the control solution the currents recover, indicating a reversible block of the channel. The voltage-dependent block and subsequent recovery of the currents can also be clearly seen from the current-voltage relationships shown in Figure 4B.

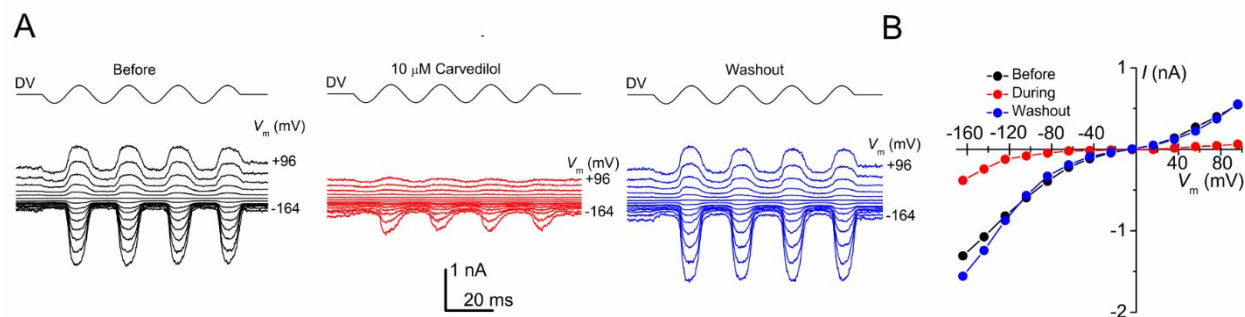


**Figure 4.** Extracellular exposure to carvedilol reduces OHC MET currents at all potentials, with the reduction most pronounced at intermediate and depolarized potentials. (A) MET currents recorded from a basal-coil OHC between -164 and +96 mV before, during and after exposure to 10  $\mu$ M carvedilol. (B) Current-voltage relationships of the currents shown in A reveal the current block at all potentials during carvedilol exposure and the reversibility of the block following washout. The capacitance of the cell was 7.4 pF.

Average normalized current voltage relationships derived from all cells recorded from at the three different concentrations tested, normalized to the maximum control current at +96 mV for each cell, demonstrate both the increase in the block with increasing compound concentration and the voltage-dependence of the block, with the strongest block observed at the intermediate and depolarized potentials (Figure 5A).



1.5  $\mu\text{M}$ , Hill coefficient 0.9. (D) Variations in the half-blocking concentration and Hill coefficient at each membrane potential.

Some recovery of the currents can be seen at the extreme depolarized potentials (+96 mV), with even more pronounced recovery at the extreme hyperpolarized potentials (-164 mV). This recovery with hyperpolarization is more evident from the average fractional block curves showing the current during carvedilol superfusion relative to the control current at each membrane potential (Figure 5B). Maximum block is seen at the intermediate membrane potentials for each concentration of carvedilol with some recovery at depolarized potentials and even greater recovery at the extreme hyperpolarized potentials. This recovery at the hyperpolarized potentials is indicative of a permeant blocker with the compound, positively charged at physiological pH (calculated  $\text{pK}_a = 8.7$ ), being drawn into the cell by the electrical driving force and therefore reducing the block of the channel. Fitted curves are to a two-barrier, one-binding site model of the MET channel permeation pathway. Dose-response curves for the extracellular block of the MET channels by carvedilol were generated at each membrane potential and fitted with equation (1) described in the experimental section. The dose-response curves derived from the currents at -164 mV, +16 mV and +96 mV are shown in Figure 5C. The  $K_D$  values range from 6.3  $\mu\text{M}$  at -164 mV to 0.1  $\mu\text{M}$  at +16 mV, close to the potential at which the block was strongest (+12.8 mV). The  $K_D$  at -84 mV was 2.0  $\mu\text{M}$ , lower than that previously reported for the AG dihydrostreptomycin (DHS), which was found to have a  $K_D$  of 7.0  $\mu\text{M}$  at -84 mV in 1.3 mM extracellular  $\text{Ca}^{2+}$ ,<sup>7</sup> indicating that carvedilol is a relatively high affinity blocker of the MET channel. Figure 5D reports the  $K_D$  and Hill coefficient values for each dose-response curve showing the strongest interaction near +16 mV. The Hill coefficients ranged from 0.5 to

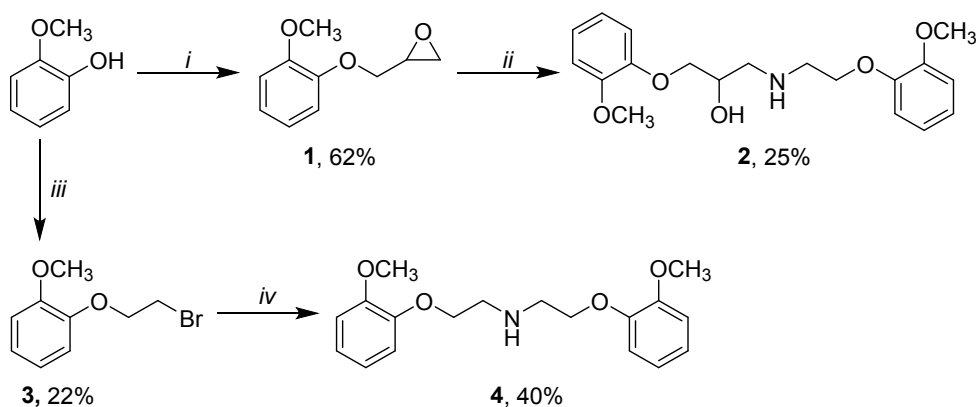
1.3 suggesting that two molecules may interact with the channel, potentially showing negative cooperativity.<sup>26</sup>

These results demonstrate that carvedilol is a relatively high-affinity permeant blocker of the MET channel and consistently protects OHCs from AGs damage at 10 and 20  $\mu$ M. However, *in vitro*, it appears to be cytotoxic at higher concentrations.

## Chemistry

Driven by these results, we decided to investigate the potential of carvedilol as potential chemical starting point for future drug development. We aimed at enhancing its protective effect in mouse cochlear cultures, increasing its block of the MET channel current and reducing the cytotoxicity observed *in vitro*. We decided to investigate its structure by modifying the carbazole moiety, the anisole ring and the  $\beta$ -hydroxyl amino group. We firstly synthesised compound **2**, by substituting the carbazole with anisole. The synthesis involved the preparation of **1** by coupling 2-methoxyphenol and 2-(bromomethyl)oxirane followed by epoxide ring opening with commercially available 2-(2-methoxyphenoxy)ethanamine in ethylene glycol dimethyl ether at 80 °C providing the desired compound in moderate yield.

## Scheme 1

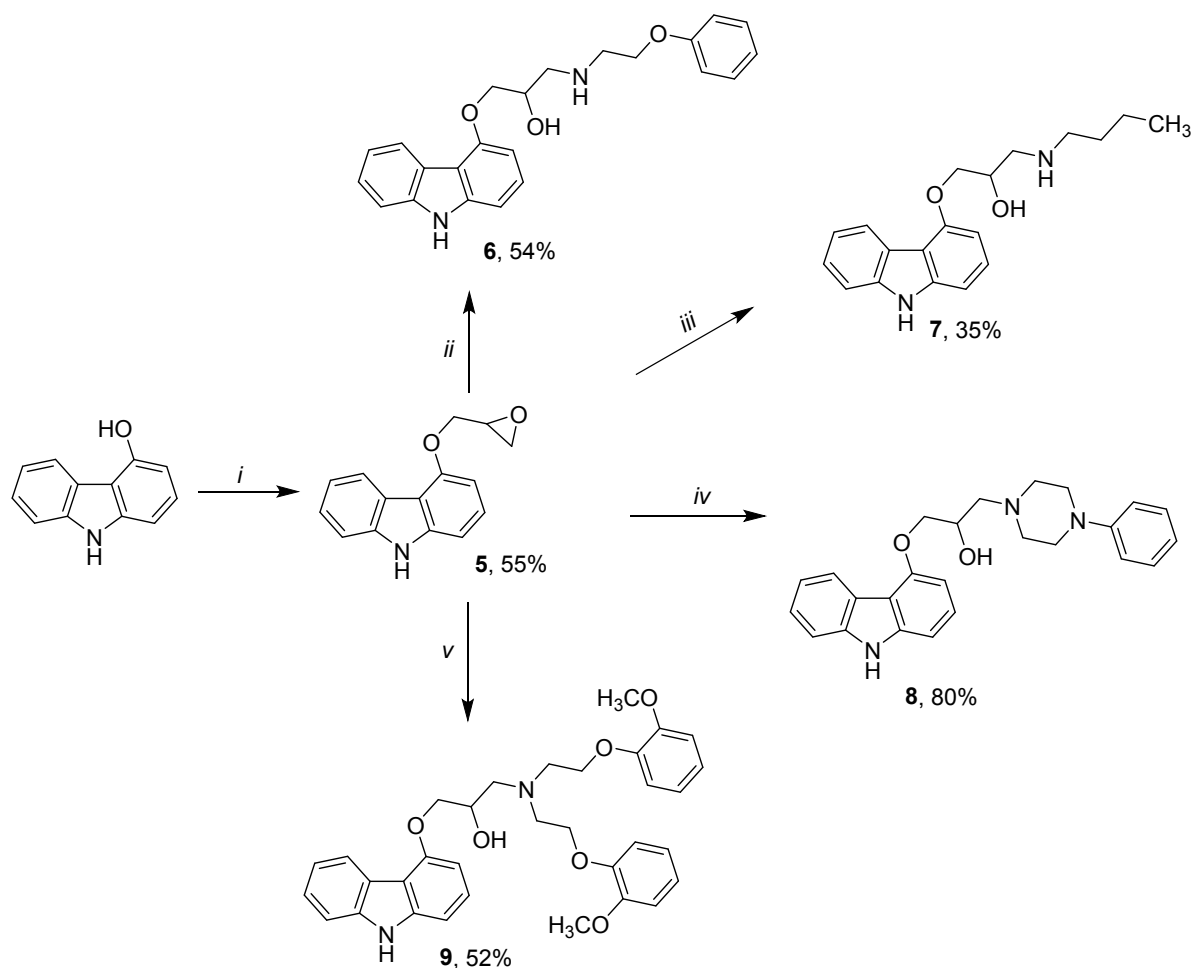


Reagents and conditions: (i) 2-(bromomethyl)oxirane, anhydrous  $K_2CO_3$ , DMF, 70 °C, 6 h; (ii) 2-(2-methoxyphenoxy)ethanamine, ethylene glycol dimethyl ether, 80 °C, 6 h; (iii) 1,2-dibromoethane, NaOH, water, reflux, 3 h; (iv) 2-(2-methoxyphenoxy)ethanamine, TEA, THF, 65 °C, 6 h

In parallel, to simplify the structure of carvedilol and likely removing its interactions with adrenergic receptors, we investigated the requirement for the  $\beta$ -hydroxyl amino group by evaluating compound **4**, which was prepared by coupling 2-(2-methoxyphenoxy)ethanamine and **3**, which was previously made by reacting 2-methoxyphenol with 1,2-dibromoethane.

## Scheme 2





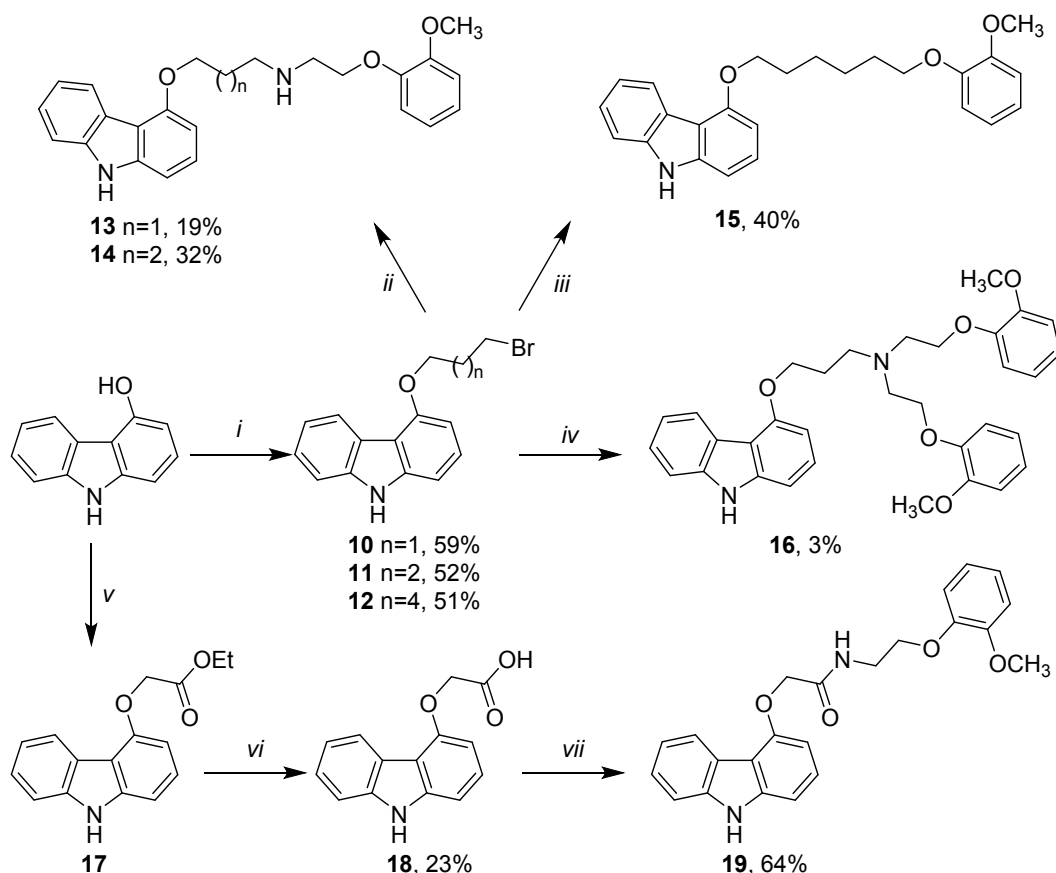
Reagents and conditions: (i) 2-(bromomethyl)oxirane, NaOH, water, DMSO, 45 °C, 16 h; (ii) 2-phenoxyethanamine, ethylene glycol dimethyl ether, 80 °C, 24 h; (iii) butan-1-amine, ethylene glycol dimethyl ether, 80 °C, sealed tube, 24 h; (iv) phenylpiperazine, ethanol, 65 °C, 16 h; (v) **4**, ethylene glycol dimethyl ether, 80 °C, sealed tube, 48 h.

We then investigated the role of the anisole ring by simplifying to a simple phenol **6** and an aliphatic chain **7**; the role of the basic centre by inserting a cyclic tertiary amine (phenylpiperazinyl) **8** and a tertiary amine bearing two 2-(2-methoxyphenoxy)ethanamine moieties **9**. These compounds are prepared starting from the common intermediate **5**, which is made by reacting 4-hydroxycarbazole with 2-(bromomethyl)oxirane in good yield. The epoxide ring is then opened by the appropriate amine using ethylene glycol dimethyl ether as solvent for **6**, **7**

1 and **9** in moderate to good yield, while in the case of **8** ethanol was used as solvent affording the  
2 desired compound in 80% yield.

3 We then investigated the role of the hydroxyl group by preparation of **13**, the carbazole-amine  
4 linker **14**, removing the  $\beta$ -hydroxyl amine by linking the carbazole and the anisole rings via a six  
5 carbon chain **15** and removing the basic centre by the introduction of an amidic bond **19**. Based  
6 on the biological data obtained with compounds **9** and **13**, we combined these modifications to  
7 make compound **16**. For the synthesis, 4-hydroxycarbazole was reacted with either 1,3-  
8 dibromopropane, 1,4-dibromobutane or 1,6-dibromohexane to give compounds **10-12**  
9 respectively. Compounds **10** and **11** were coupled with 2-(2-methoxyphenoxy)ethanamine  
10 yielding **13** and **14**, while compound **12** was coupled with 2-methoxyphenol to give **15** in  
11 moderate yield. Compound **16** was obtained by coupling **10** with **4**. For the preparation of amide  
12 analogue **19**, 4-hydroxycarbazole was reacted with ethyl chloroacetate to afford the ester **17**,  
13 which was hydrolysed with aqueous sodium hydroxide providing the acid **18**. Coupling with 2-  
14 (2-methoxyphenoxy)ethanamine was performed under standard amide coupling conditions using  
15 1-hydroxybenzotriazole (HOBt) and N-(3-dimethylaminopropyl)-N'-ethylcarbodiimide (EDC)  
16 affording the desired compound **19** in good yield.

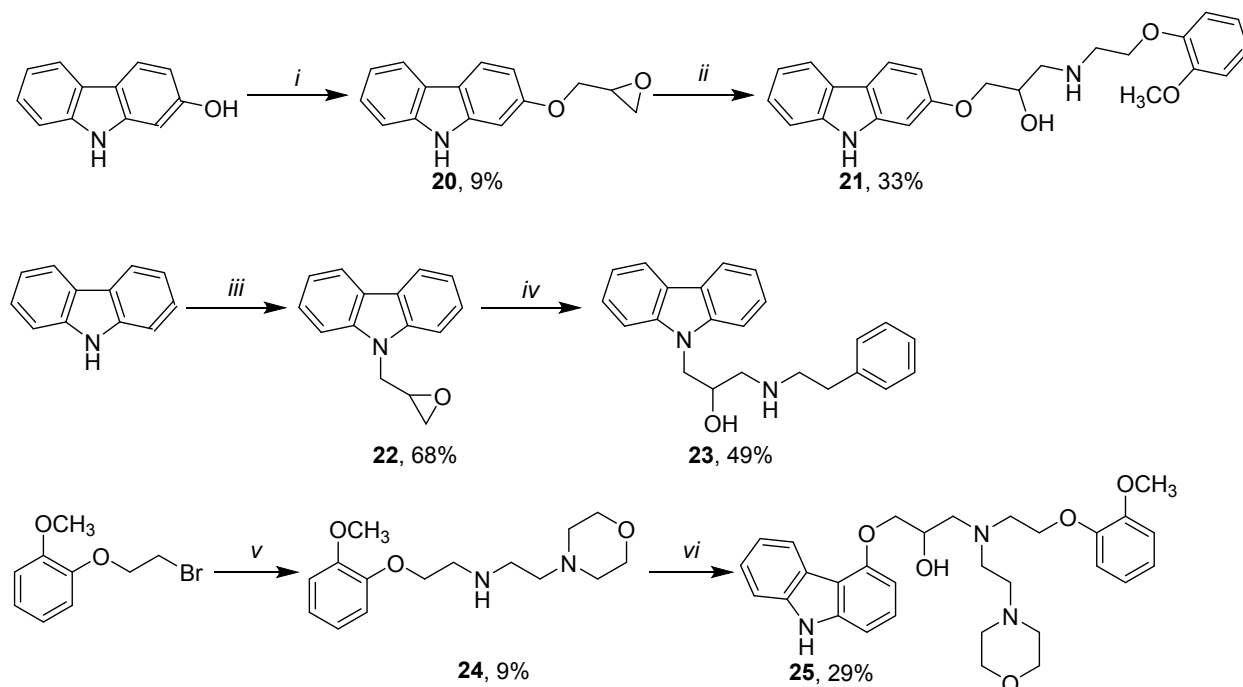
## Scheme 3



Reagents and conditions: (i) 1,3-dibromopropane for **10**, 1,4-dibromobutane for **11**, 1,6-dibromohexane for **12**, KOH, acetonitrile, rt, 5-18 h; (ii) 2-(2-methoxyphenoxy)ethanamine, anhydrous K<sub>2</sub>CO<sub>3</sub>, DMF, rt, 16 h for **13**; 2-(2-methoxyphenoxy)ethanamine, TEA, THF, 65 °C, 24 h for **14**; (iii) 2-methoxyphenol, KOH, acetonitrile, rt, 66 h; (iv) **4**, K<sub>2</sub>CO<sub>3</sub>, DMF, rt, 36 h; (v) ethyl chloroacetate, K<sub>2</sub>CO<sub>3</sub>, acetone, reflux, 16 h; (vi) 1N aqueous NaOH, THF, rt, 16 h; (vii) 2-(2-methoxyphenoxy)ethanamine, HOBT, EDC·HCl, DIPEA, DMF, rt, 16 h.

We then investigated two isomers of carvedilol: the 2-hydroxycarvedilol derivative **21**, which was obtained by opening the epoxide ring of compound **20** with 2-(2-methoxyphenoxy)ethanamine providing the desired compound **21** in moderate yield (Scheme 4); and the 1-carbazole isomer by directly linking the side chain to the nitrogen of the carbazole ring. Firstly, carbazole was reacted with epichlorohydrin to yield compound **22** followed by epoxide ring opening using 2-phenylethylamine obtaining compound **23** in 49% yield.

# Scheme 4



Reagents and conditions: (i) 2-(bromomethyl)oxirane, sodium hydroxide, water, DMSO, 45 °C, 16 h; (ii) 2-(2-methoxyphenoxy)ethanamine, ethanol, 65 °C, 16 h; (iii) 2-(bromomethyl)oxirane, potassium hydroxide, acetonitrile, rt, 20 h; (iv) 2-phenylethylamine, ethanol, 65 °C, 16 h; (v) 4-(2-aminoethyl)morpholine, TEA, THF, 65 °C, 4 h; (vi) 4-(oxiran-2-ylmethoxy)-9H-carbazole, ethanol, 65 °C, 16 h.

Finally, to improve the solubility of compound **9**, we designed compound **25** in which one of the 2-methoxyphenoxy group was substituted with a morpholine ring. Compound **3** was reacted with commercially available 4-(2-aminoethyl)morpholine to obtain compound **24** which was then coupled with **5** to give the desired compound **25** in 29% yield.

## Carvedilol derivatives: protective abilities and MET channel block

The newly synthesised compounds were screened to assess their protective ability against 5  $\mu$ M gentamicin using mouse cochlear cultures initially at 20  $\mu$ M, a concentration at which carvedilol

1 provided full protection and was not cytotoxic. Any compounds that showed full or partial  
2 protection were then screened at lower concentrations to establish their minimal protective  
3 concentration. We initially designed and synthesised 6 compounds aimed at evaluating the  
4 chemical moiety essential for the interaction with the MET channel, these include: modification  
5 at the carbazole (**2** and **4**) and anisole (**6** and **7**) rings, the removal of the hydroxyl group (**13**) and  
6 the introduction of a second 2-phenoxyethyl moiety to form a tertiary amine (**9**). When tested at  
7 20  $\mu$ M (Figure 6), compounds **2** and **4** lacking the carbazole moiety provided no protection  
8 (Figure 6C and D), while compound **6** with a phenyl group instead of the anisole proved to be  
9 generally cytotoxic (Figure 6E). Compound **9**, bearing two 2-methoxyphenoxyethyl moieties,  
10 offered only partial protection (Figure 6G) while compounds **7** and **13** consistently protected  
11 against OHC loss (Figure 6F and H). As a reference, control cochlear cultures exposed to 0.5%  
12 DMSO (Figure 6A) and 5  $\mu$ M gentamicin (Figure 6B) as well as quantification for both controls  
13 and cultures exposed to compounds (Figure 6I) are included.

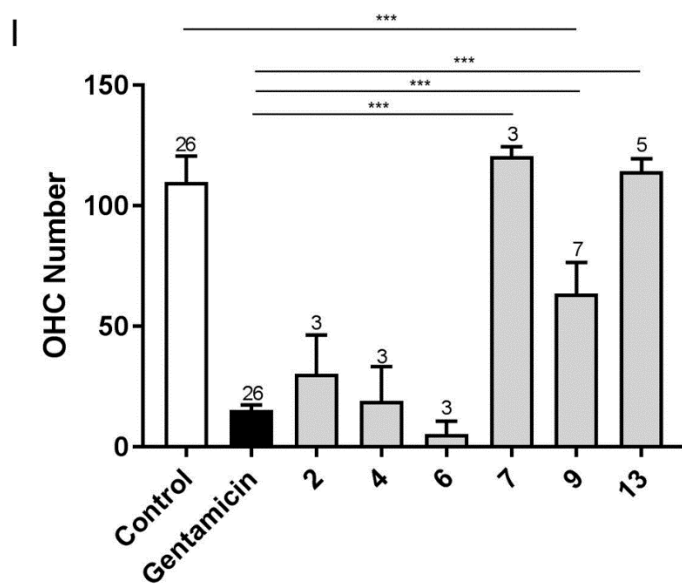
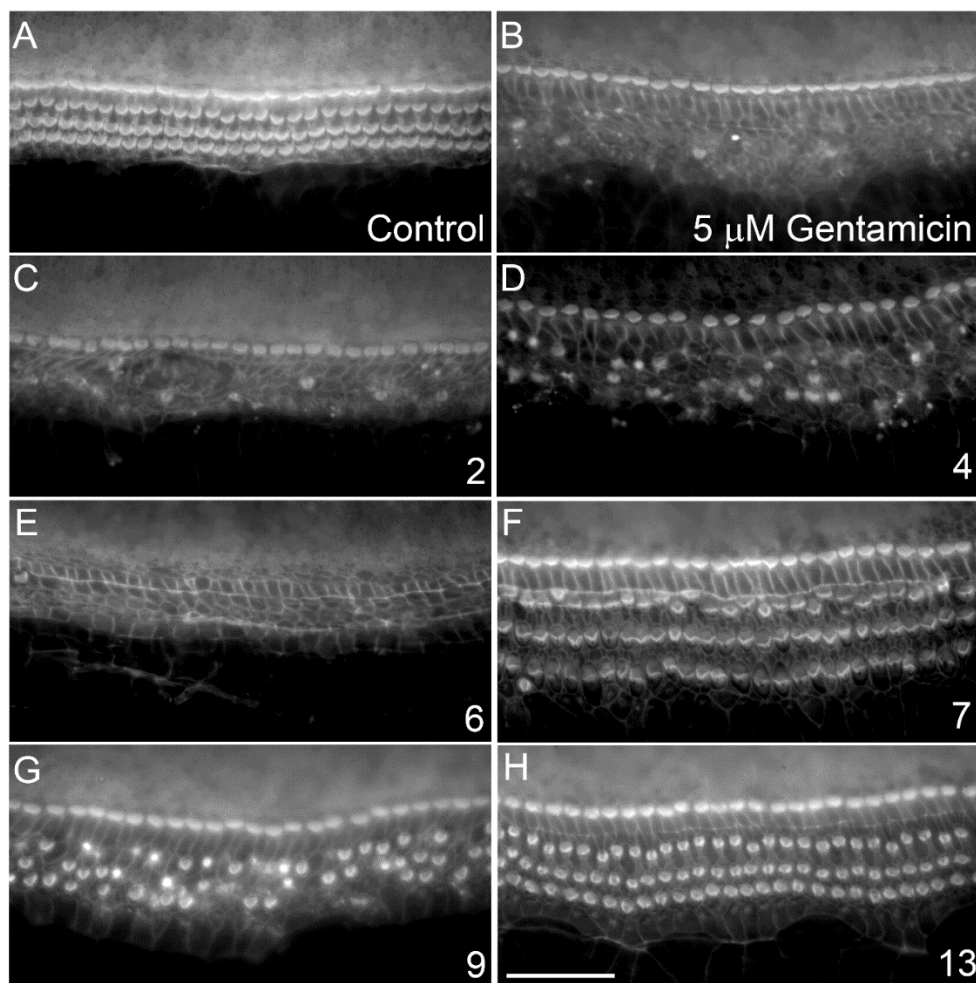


**Figure 6.** Otoprotective effect of compounds **2**, **4**, **6**, **7**, **9**, and **13** in cochlear cultures against 5  $\mu$ M gentamicin. (A) A control culture exposed to 0.5% DMSO for 48 h. (B) A culture exposed to 5  $\mu$ M gentamicin + 0.5% DMSO for 48 h. (C-H) Cultures exposed to 5  $\mu$ M gentamicin for 48 h + 20  $\mu$ M: (C) **2**, (D) **4**, (E) **6**, (F) **7**, (G) **9**, (H) **13**. Scale bar is 50  $\mu$ m. (I) Quantification of OHC survival for the control and compound exposed cultures.

The three derivatives (**7**, **9** and **13**) that showed partial or full protection at 20  $\mu$ M were subsequently tested at 10 and 5  $\mu$ M against 5  $\mu$ M gentamicin. Only compound **13** provided full protection at 5  $\mu$ M (as well as at 10  $\mu$ M), showing an improvement compared to the parent compound carvedilol which was only partially protective at 5  $\mu$ M (Figure 7A-E). As stated before, in the control condition some 110 OHCs were present in each cochlear segment, reducing to 15 OHCs following exposure to 5  $\mu$ M gentamicin. Additional exposure to 5  $\mu$ M carvedilol increased the average number of surviving OHCs to 66 (54% protection), whereas 5  $\mu$ M compound **13** resulted in 99 surviving OHCs (88% protection) (Figure 7E).

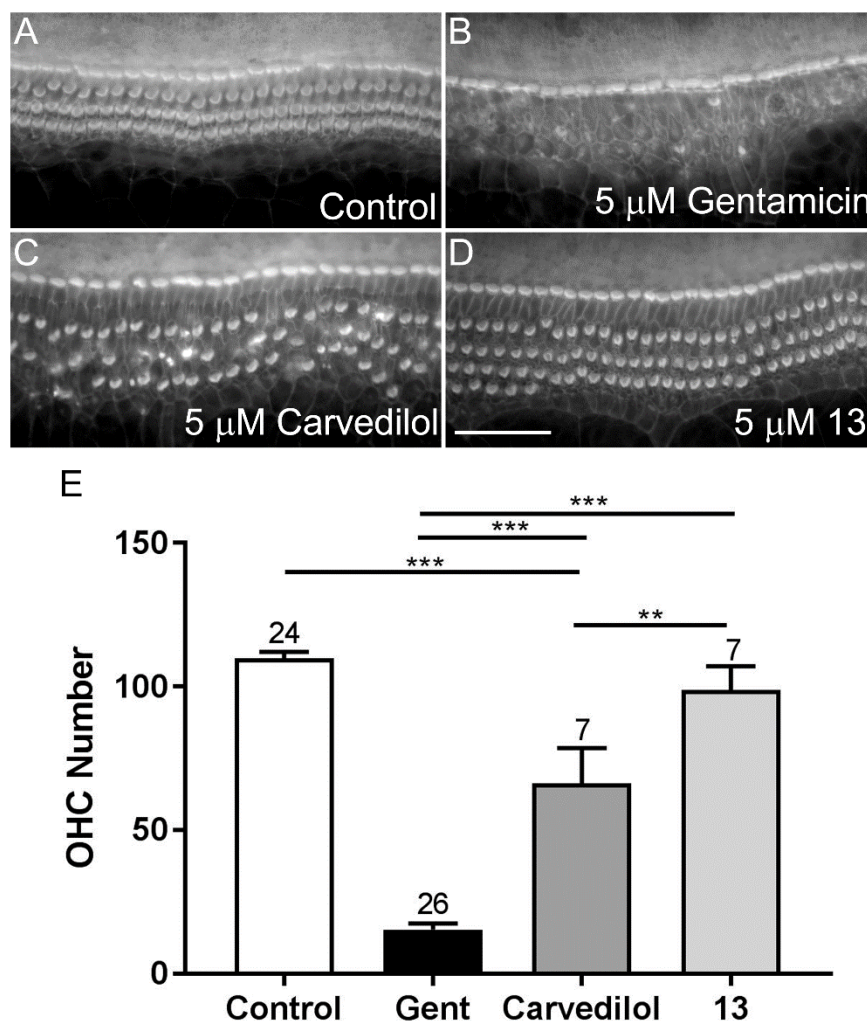


**Figure 7.** When tested at 5  $\mu$ M against 5  $\mu$ M gentamicin, compound **13** showed a greater otoprotective effect. (A) A control culture exposed to 0.5% DMSO for 48 h. (B) A culture exposed to 5  $\mu$ M gentamicin + 0.5% DMSO for 48 h. (C-D) Cultures exposed to 5  $\mu$ M gentamicin for 48 h + 5  $\mu$ M: (C) carvedilol or (D) compound **13**. Scale bar is 50  $\mu$ m. (E) Quantification of OHC survival for the control and compound-exposed cultures.

When tested alone **13** showed similar toxicity characteristics to carvedilol, proving toxic to OHCs at concentrations  $\geq 30$   $\mu$ M and affecting the IHC and OHC bundle morphology at 20  $\mu$ M.



Contrary to carvedilol, **13** was not toxic at 30  $\mu\text{M}$  when tested together with 5  $\mu\text{M}$  gentamicin, but it did also affect IHC and OHC bundle morphology (data not shown).

In conjunction with assessing the protective abilities of these 6 compounds, potential interactions with the MET channel were investigated by recording MET currents from OHCs before and during exposure to 10  $\mu\text{M}$  of each compound. Figure 8 shows fractional block of the currents during compound exposure relative to the control currents at each membrane potential revealing that two compounds **4** (magenta) and **2** (blue) have limited interaction with the channel at this concentration.

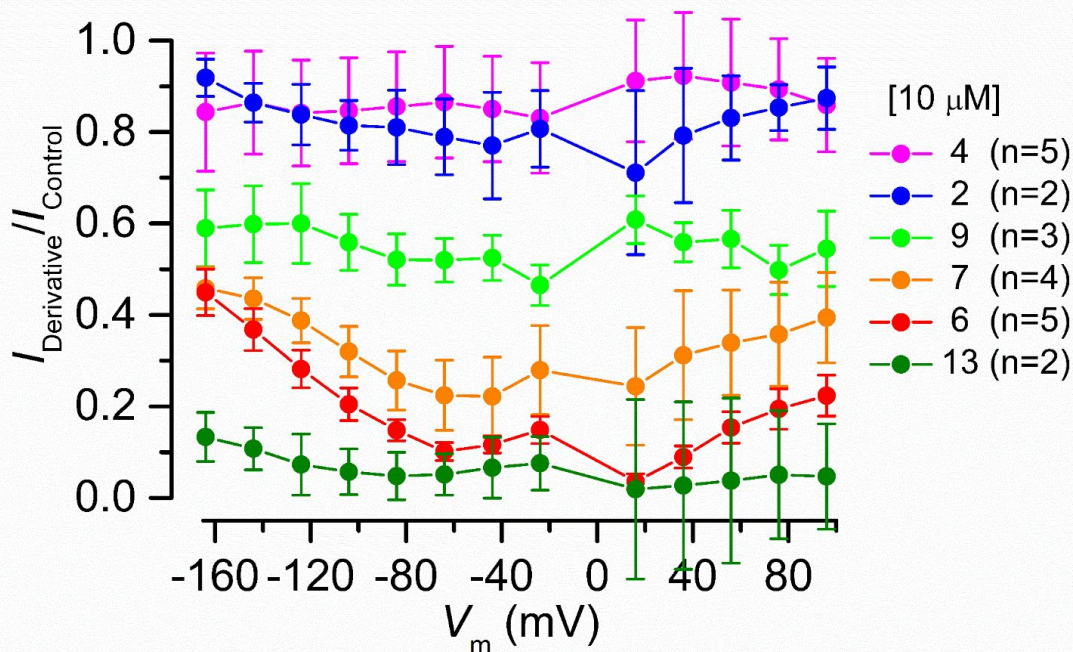


**Figure 8.** Compounds **2**, **4**, **6**, **7**, **9** and **13** show varying degrees of inhibition of the MET currents. Fractional block plots of the currents recorded during exposure to 10  $\mu\text{M}$  of each derivative relative to the control currents at each membrane potential.

1 The poor interaction of compounds **2** and **4** with the MET channel corresponded to the lack of  
2 protection observed for these compounds at 20  $\mu$ M, providing further evidence that the  
3 protection offered by carvedilol may come through a block of the MET channel. In addition,  
4 these results indicate the need for the carbazole moiety to allow the interaction with the channel.  
5 Compound **9** (bright green), which offered only a partial protection at 20  $\mu$ M, showed  
6 approximately 40% block of the MET current at all membrane potentials with no release at  
7 extreme hyperpolarized potentials suggesting this compound may act as a non-permeant blocker.  
8 Compounds **6** (red) and **7** (orange) were strong MET channel blockers at 10  $\mu$ M with a blocking  
9 profile similar to carvedilol giving approximately 50-60% block of the current at -164 mV, the  
10 most relevant physiological potential. Interestingly, compound **13** (dark green) was the most  
11 effective MET channel blocker of this series providing almost 100% block of the MET current at  
12 all membrane potentials. This result is also in accordance with its protective effect, as **13** showed  
13 protection of the OHCs from gentamicin damage at concentrations down to 5  $\mu$ M. This result  
14 again suggests that the protection observed is due to a block of the MET channels, reducing the  
15 entry of gentamicin into the cells. Compounds **6**, **7** and **13** appear to be permeant blockers of the  
16 MET channel, indicated by the release of the block at the extreme hyperpolarized potentials, and  
17 in the case of compound **13** the release of the block was less pronounced than with carvedilol  
18 itself.

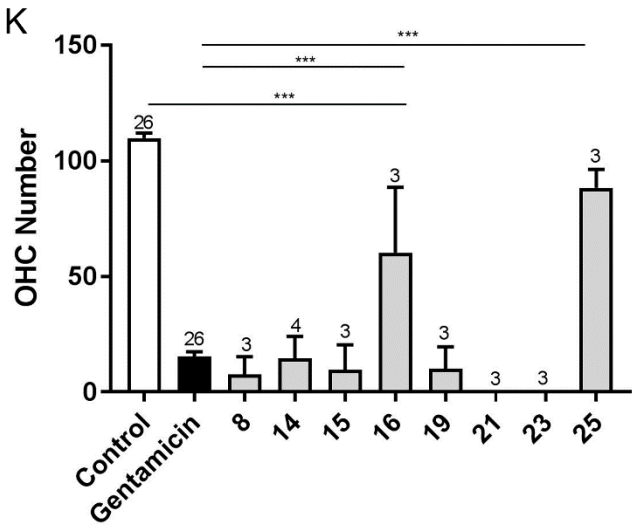
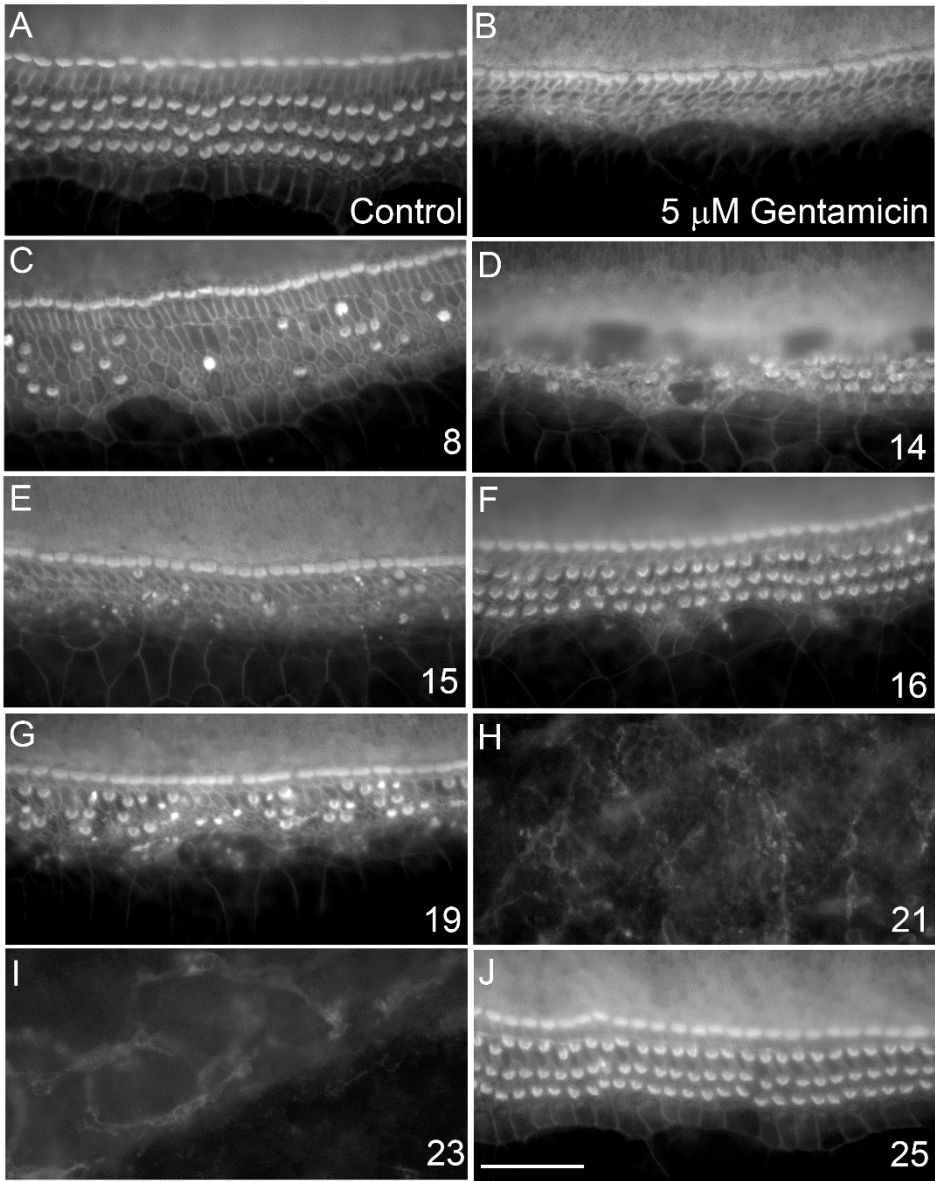


**Figure 9.** Otoprotective effect of compounds **8**, **14**, **15**, **16**, **19**, **21**, **23** and **25** in cochlear cultures against 5  $\mu$ M gentamicin. (A) A control culture exposed to 0.5% DMSO for 48 h. (B) A culture exposed to 5  $\mu$ M gentamicin + 0.5% DMSO for 48 h. (C-J) Cultures exposed to 5  $\mu$ M gentamicin for 48 h + 20  $\mu$ M: (C) **8**, (D) **14**, (E) **15**, (F) **16**, (G) **19**, (H) **21**, (I) **23**, (J) **25**. Scale bar is 50  $\mu$ m. (K) Quantification of hair cell survival for the control and cultures exposed to compounds.

A further 7 compounds (**8**, **14**, **15**, **19**, **21**, **23** and **25**) were then designed and synthesised in an attempt to improve their protective abilities and physicochemical properties. Of these, **14**, **15**, **21** and **23** were generally cytotoxic when tested at 20  $\mu$ M against 5  $\mu$ M gentamicin (Figure 9D, E, H and I respectively), **19** and **8** offered no protection (Figure 9C and G respectively), and **25** was consistently protective (Figure 9J). When tested at 10  $\mu$ M, **25** was protective in 2 out of 4 screens but offered no protection at 5  $\mu$ M (data not shown). MET channel interactions were subsequently investigated for derivative **25** that showed protection at 20  $\mu$ M and partial protection at 10  $\mu$ M. The resulting fractional block plot reveals that at a concentration of 10  $\mu$ M, **25** blocks the MET channel at all membrane potentials (Figure 10). However, the degree of block is far less than that observed for carvedilol and **13** suggesting this derivative has a reduced affinity for the channel. Combining the desired characteristics of a non-permeant MET channel blocker (**9**) with a high-affinity blocker (**13**), we designed, synthesised and tested a further derivative (**16**). This compound was found fully protective at 20  $\mu$ M against 5  $\mu$ M gentamicin on only one out of three occasions (Figure 9F), with no protection in the other two trials. The lack of consistency with the data was probably caused by the poor solubility of the compound. When tested at 10  $\mu$ M, compound **16** did not offer any protection (data not shown). When tested in our



electrophysiology assay, compound **16** showed limited interaction with the MET channel at both 3 and 10  $\mu\text{M}$  (data not shown).

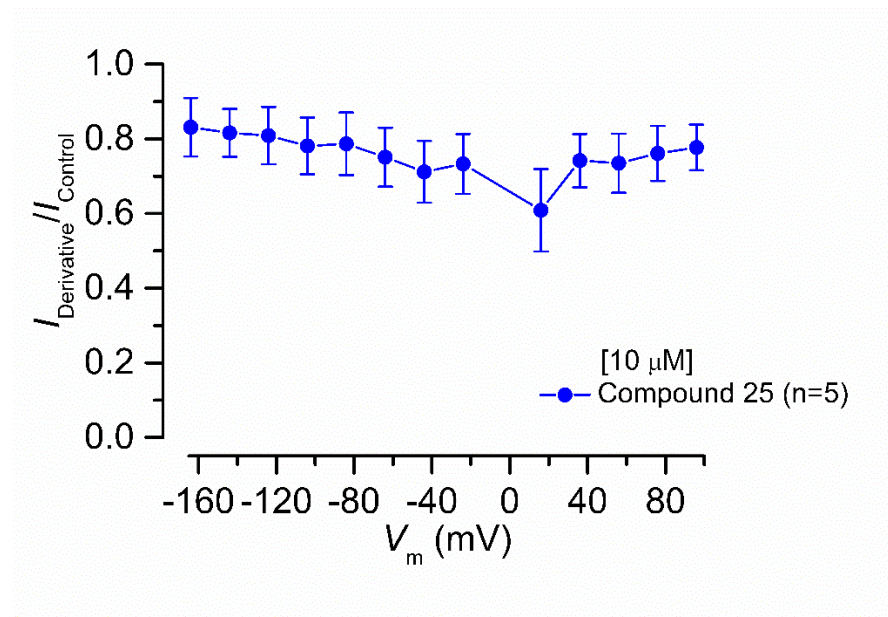


**Figure 10.** The fractional block plot for compound **25** (10  $\mu\text{M}$ ). The size of the current during exposure to the compound relative to the control current at each membrane potential reveals compound **25** has a low affinity for the MET channel.

### Assessing the protective effect and MET channel properties of adrenergic receptor and calcium channel blockers.

We then proceeded to investigate whether the adrenergic ( $\alpha$  and  $\beta$ ) receptors, primary pharmacological targets of carvedilol, play a role in its otoprotective abilities. We tested the non-selective  $\beta$ -blocker propranolol **26**, the selective  $\beta_1$ -blocker CGP20712 **27**, the selective  $\alpha_1$ -blocker naftopidil **28**, and the non-selective adrenergic blocker and calcium channel-blocker verapamil **29** (Figure 11).

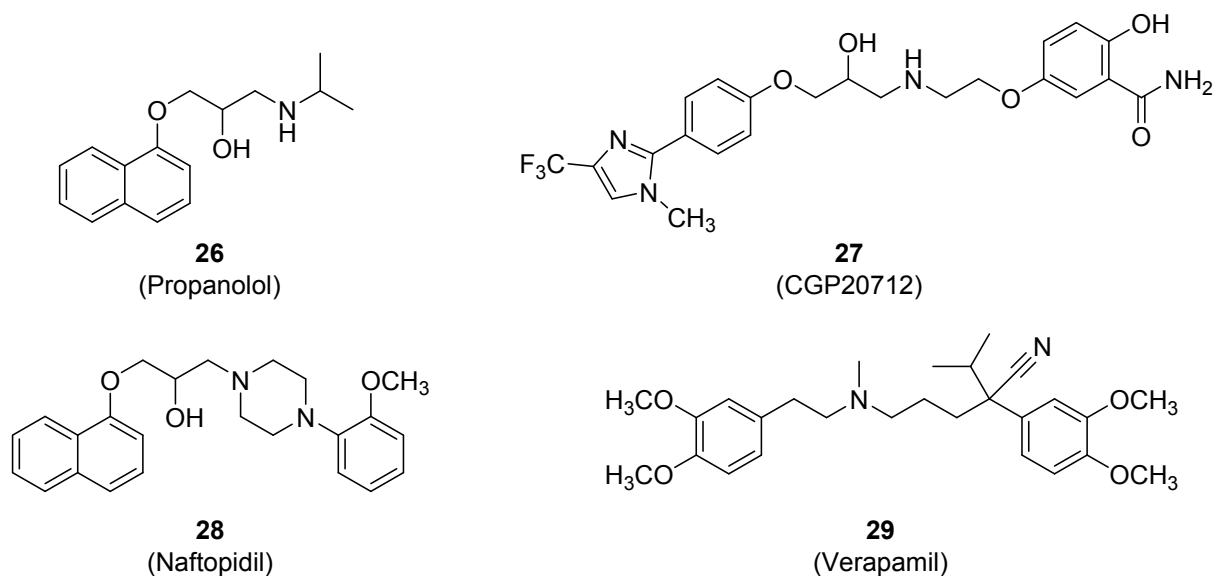


**Figure 11.** Chemical structure of other adrenergic blockers (**26-28**) and calcium channel-blocker **29** used in this study.

Compounds **26**, **27** and **29** did not offer any protection against 5  $\mu$ M gentamicin when tested at 20  $\mu$ M (Figure 12 C, D, and F respectively), while **28** proved to be partially effective under the same conditions (Figure 12 E, G). However, when the test concentration was lowered to 10  $\mu$ M, compound **28** did not protect cochlear culture hair cells against gentamicin damage (data not shown).

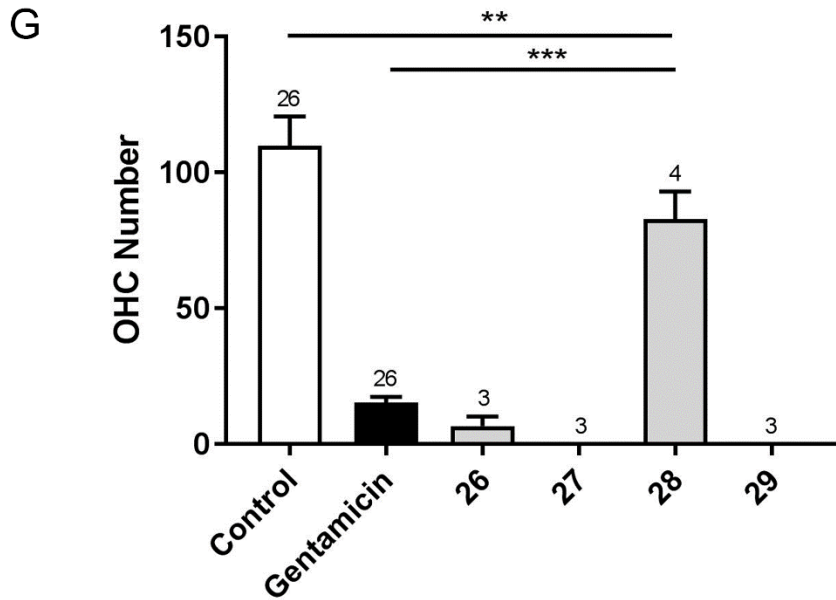
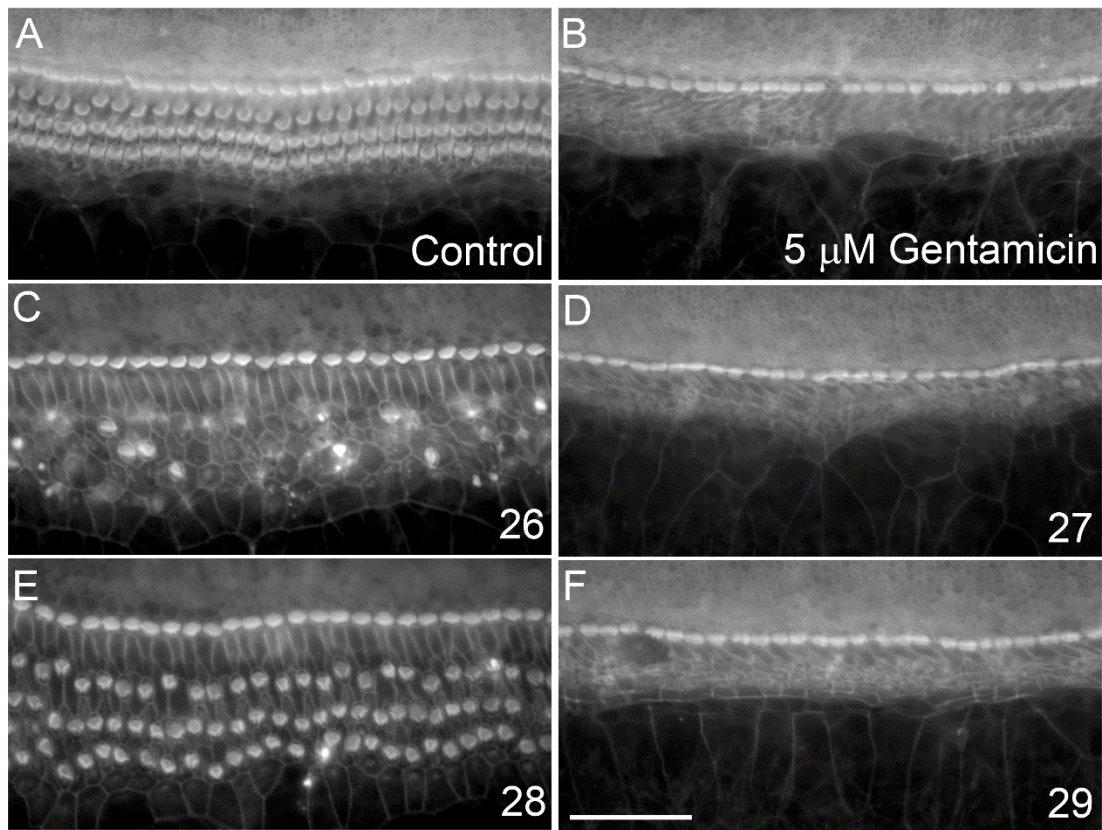
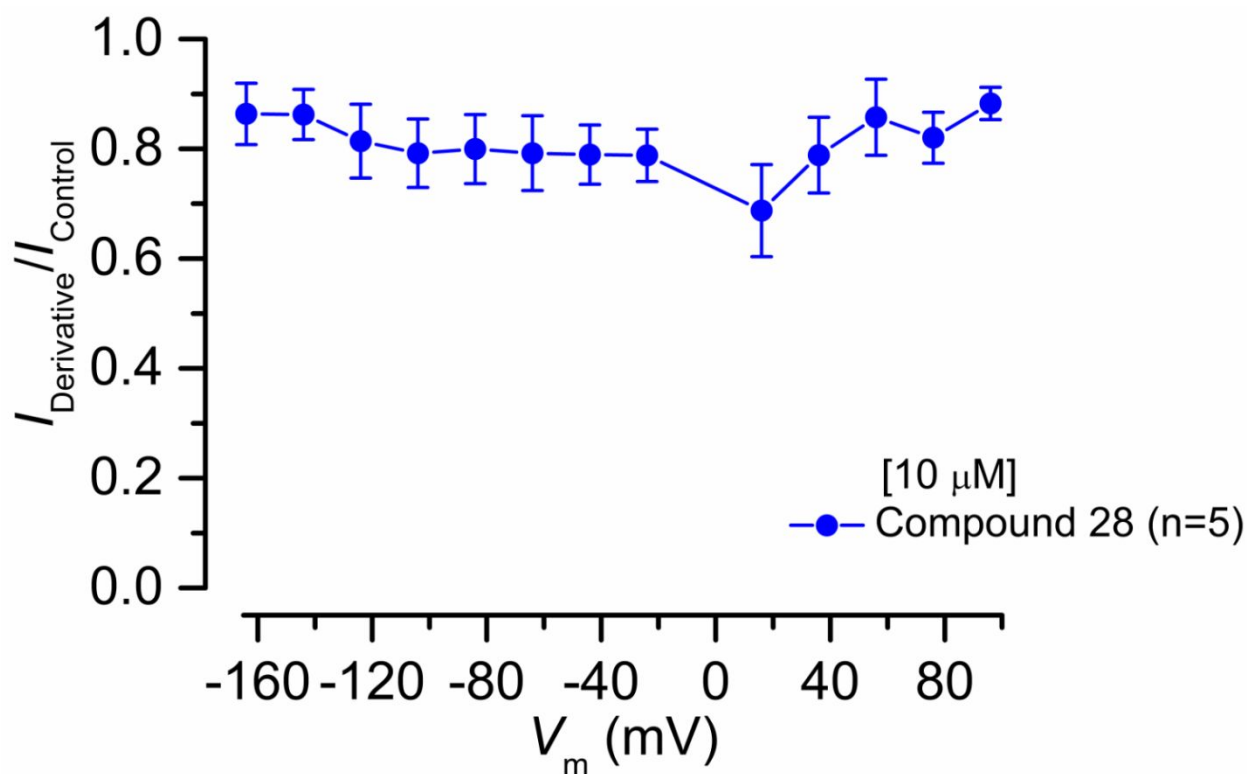


**Figure 12.** Otoprotective effect of compounds **26**, **27**, **28**, and **29** in cochlear cultures against 5 μM gentamicin. (A) A control culture exposed to 0.5% DMSO for 48 h. (B) A culture exposed to 5 μM gentamicin + 0.5% DMSO for 48 h. (C-F) Cultures exposed to 5 μM gentamicin for 48 h +

1 20  $\mu$ M: (C) **26**, (D) **27**, (E) **28**, (F) **29**. (G) Quantification of hair cell survival for the control and  
2 compound exposed cultures. Scale bar is 50  $\mu$ m.

3 We subsequently investigated the affinity of the partially protective compound **28** for the MET  
4 channel. This compound did not interact strongly with the MET channel, revealed from the  
5 fractional block plot shown in Figure 13.



6  
7 **Figure 13.** The fractional block plot for compound **28**. The size of the current during exposure to  
8 the compound relative to the control current at each membrane potential reveals compound **28**  
9 has a low affinity for the MET channel.

11 **Electrophysiological properties of compound 13: a strong permeant MET channel blocker**



The cochlear culture protection assay revealed that the carvedilol derivative **13**, at a concentration of 5  $\mu\text{M}$ , displayed a consistent protective effect against 5  $\mu\text{M}$  gentamicin. When tested on its own compound **13** appears to be cytotoxic at 30  $\mu\text{M}$ . However, when tested in the presence of 5  $\mu\text{M}$  gentamicin compound **13** is not toxic, suggesting a competitive interaction at the level of the MET channel that may effectively reduce the cytotoxic effects of both compounds. In order to compare MET channel interactions between compound **13** and carvedilol, MET currents were recorded before and during **13** exposure at 1, 3 and 10  $\mu\text{M}$  and the resulting current-voltage relationships, fractional block curves and dose-response curves generated (Figure 14).

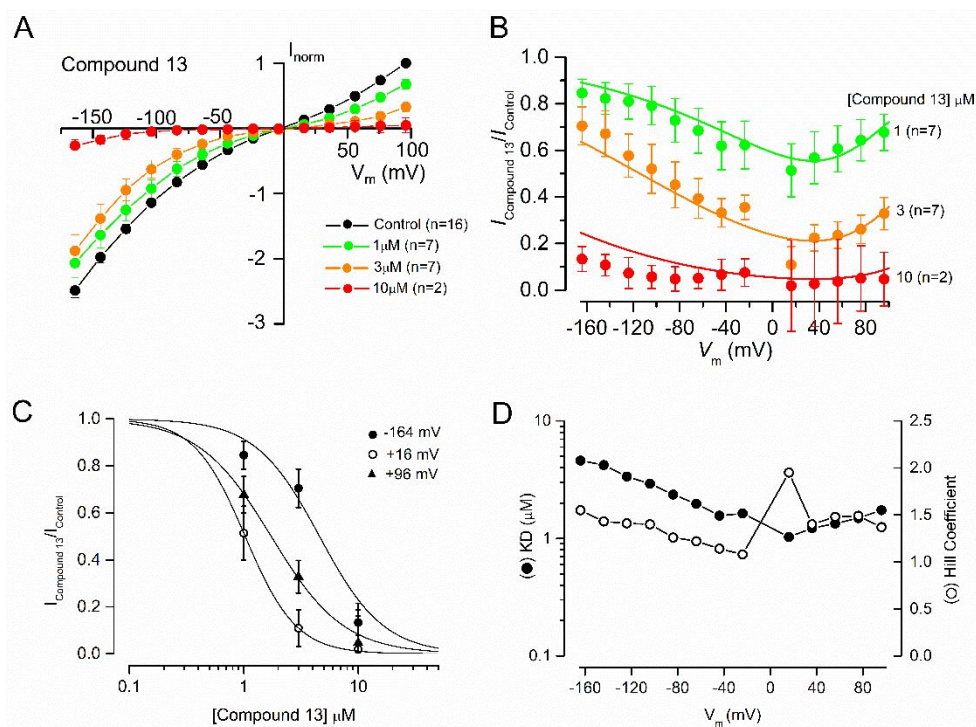


**Figure 14.** Compound **13** acts as a permeant blocker of the MET channel, with similar blocking properties to carvedilol. (A) Average normalized current-voltage relationships for the peak MET

currents recorded before and during exposure to 1, 3 and 10  $\mu\text{M}$  **13**. (B) Fractional block curves for compound **13** tested at 1, 3 and 10  $\mu\text{M}$  reveal it is a permeant MET channel blocker. Fitting parameters are  $\Delta E$  -2.22 kT;  $E_b$  -21.3 kT;  $\delta_b$  0.71;  $z$  1.0;  $\delta_b$  0.71; Hill coefficient 1.4. Maximum block occurs at +33.9 mV. (C) Dose-response curves derived from the currents recorded at -164, +16 and +96 mV and fit with equation (1). -164 mV:  $K_D$  4.6  $\mu\text{M}$ , Hill coefficient 1.6; +16 mV:  $K_D$  1.0  $\mu\text{M}$ , Hill coefficient 2.0; +96 mV:  $K_D$  1.7  $\mu\text{M}$ , Hill coefficient 1.4. (D) Variations in the half-blocking concentration and Hill coefficient at each membrane potential.

From the average normalized current-voltage relationships (Figure 14A) and the fitted average fractional block curves (Figure 14B) it can be seen that the block of the channel by **13** is very similar to that of carvedilol, with the maximum block seen at the intermediate potentials and release of the block at extreme depolarized and hyperpolarized potentials, indicating that this compound is also a permeant blocker of the MET channel. Dose-response curves were generated, derived from the currents at each membrane potential, and fitted with equation (1) (see Experimental Section). Figure 14C shows the curves derived from the currents at -164 mV, +16 mV and +96 mV, where the  $K_D$  values were found to be 4.6, 1.0 and 1.7  $\mu\text{M}$  respectively. The  $K_D$  at -84 mV (2.4  $\mu\text{M}$ ) is similar to that of carvedilol (2.0  $\mu\text{M}$ ) suggesting that both compounds are relatively high affinity blockers of the MET channel at a potential close to the resting potential *in vitro*. The Hill coefficients ranged from 1.1 to 2.0, suggesting there may be two or more binding sites within the channel for **13** (Figure 14D).<sup>26</sup>

## Kinetics of MET channel block for carvedilol and compound **13**

One further property of the MET channel interaction that was investigated for both carvedilol and **13** was the kinetics of the block, to determine whether or not these compounds are open channel blockers, similar to berbamine and d-tubocurarine,<sup>20</sup> or can reside in the closed channel, similar to the permeant MET channel blocker FM1-43.<sup>6</sup> The time course of the block is revealed by applying large force steps to the hair bundles both before and during exposure to the compound and recording the resulting currents. Such currents can be seen before and during exposure to carvedilol (1 and 3  $\mu$ M; Figure 15A, B) and **13** (1 and 3  $\mu$ M; Figure 15C, D). From a holding potential of -84 mV, channel opening results in rapidly activating inward currents in all conditions. During the step the currents show minimal adaptation in control conditions and an exponential decline during both carvedilol and **13** exposure. This suggests that both compounds are open channel blockers, accessing their binding site once the channel has opened. Time constants were measured from the current decline and found to be:  $18.0 \pm 5.0$  ms (1  $\mu$ M carvedilol; n=3);  $9.6 \pm 0.4$  ms (3  $\mu$ M carvedilol; n=4);  $9.9 \pm 0.9$  ms (1  $\mu$ M **13**; n=3);  $6.0 \pm 1.6$  ms (3  $\mu$ M **13**; n=3).

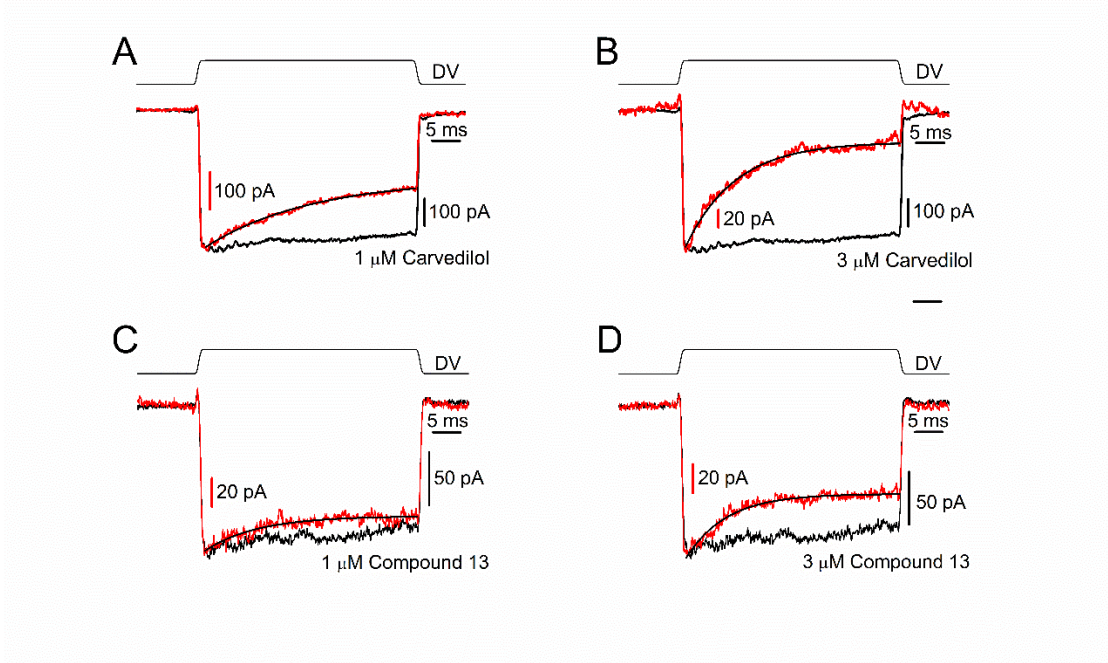


**Figure 15:** Kinetics of MET channel block mediated by carvedilol and **13** reveals both act as open channel blockers. (A-D) Currents resulting from a mechanical step delivered by the fluid-jet ( $\pm 40$  V driver voltage, DV shown above each trace), from a holding potential of  $-84$  mV, before (black trace) and during (red trace) superfusion of (A)  $1\ \mu\text{M}$  carvedilol, (B)  $3\ \mu\text{M}$  carvedilol, (C)  $1\ \mu\text{M}$  **13**, (D)  $3\ \mu\text{M}$  **13**. Currents (averaged from 10 repetitions) before and during compound exposure have been scaled and superimposed. The currents during compound superfusion were fitted with single exponentials (A)  $\tau = 19.3$  ms, (B)  $\tau = 8.6$  ms, (C)  $\tau = 10.1$  ms, (D)  $\tau = 6.9$  ms.

From these time constants, entry rates of the drug molecules into the hair cells were calculated (see Experimental Section), and their energy profiles for permeation through the MET channel pore determined (Figure 16). Both compounds bind much stronger (free energy  $E_b < -15$  kT) to the binding site in the channel pore than DHS ( $E_b -8.27$  kT at  $1.3$  mM extracellular  $\text{Ca}^{2+}$ )<sup>7</sup> and the drugs d-tubocurarine ( $-8.67$  kT) and berbamine ( $-12.0$  kT) that we evaluated before.<sup>20</sup> A consequence of this is that, unlike the other compounds, the maximum block for these monovalent cations (at physiological pH) occurs at positive membrane potentials (Figures 5B and 14B). Moreover, their permeation through the MET channels is considerably slower than DHS. For example, with  $1\ \mu\text{M}$  of compound, 80 MET channels with an open probability of  $0.1$  and a membrane potential of  $-150$  mV, the entry rates into the OHCs are  $165$  molecules/s for carvedilol and  $125$  molecules/s for **13**, compared with some  $1130$  molecules/s for DHS.<sup>7, 20</sup> For higher concentrations the entry rates started to saturate, so they never approach those for DHS (e.g. for  $100\ \mu\text{M}$  rates were  $1078$  molecules/s for carvedilol,  $998$  molecules/s for **13** and  $11,460$  molecules/s for DHS).

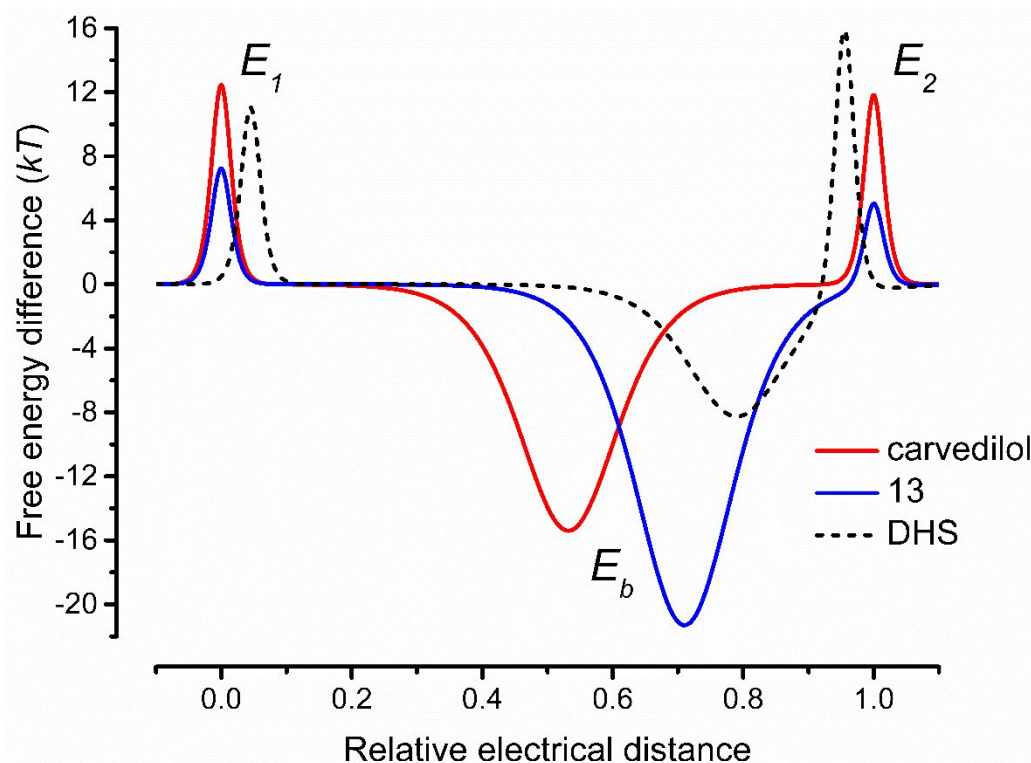


**Figure 16:** Energy profiles for MET channel permeation and block by carvedilol and **13**. Energy profiles calculated from fits to the fractional-block curves and kinetics of MET current block are shown. Values for the free energies of the binding site  $E_b$  and barriers  $E_1$  and  $E_2$  are shown in the absence of a voltage across the membrane ( $V_m = 0$  mV). The voltage-independent extracellular barrier  $E_1$ , at an electrical distance of zero, has a free energy of 12.5 kT for carvedilol and 7.23 kT for **13**. The free energy of  $E_b$  is -15.4 kT for carvedilol and -21.3 kT for **13**. The binding sites,  $\delta_b$ , are located at an electrical distance from the extracellular side of 0.53 for carvedilol and 0.71 for **13**. The intracellular barrier  $E_2$ , positioned at an electrical distance of one, is 11.8 kT for carvedilol and 5.01 kT for **13**. For comparison, the energy profile calculated before for DHS in 1.3. mM extracellular  $\text{Ca}^{2+}$  is shown (dotted line).<sup>7</sup>



### 1 Carvedilol and 13 reduce GTTR loading into hair cells

2 To further assess whether carvedilol and **13** protect sensory hair cells against AG damage by  
3 preventing the entry of the antibiotics into cells, a fluorescent gentamicin analogue (gentamicin  
4 Texas red: GTTR) was used to enable quantification of gentamicin uptake.<sup>27</sup> Pre-incubation with  
5 either 1% DMSO, 100  $\mu$ M carvedilol or 100  $\mu$ M **13** for 5 minutes prior to 0.2  $\mu$ M GTTR  
6 application resulted in significantly reduced loading of GTTR in the presence of both carvedilol  
7 and **13** relative to the DMSO control ( $p < 0.001$  in both cases) (Figure 17). A significant  
8 difference was not observed between the GTTR loading in the presence of carvedilol or **13**.  
9 These findings further suggest that both carvedilol and **13** protect against AG damage by  
10 competitively blocking the MET channel and thereby preventing AG entry into hair cells,  
11 minimising accumulation and consequent apoptosis induction.

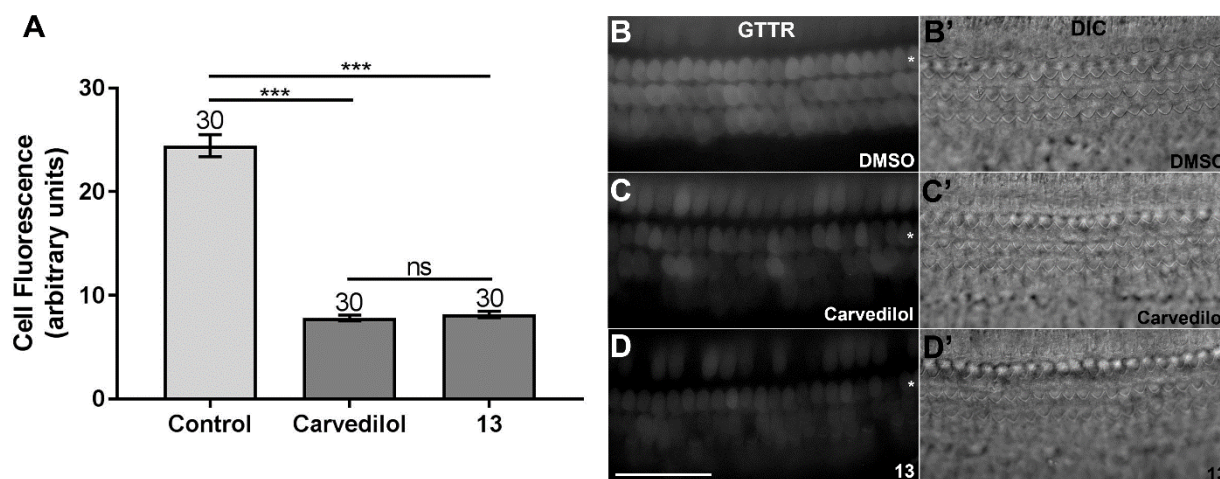


**Figure 17.** Carvedilol and **13** reduce the entry of GTTR into mouse cochlear culture hair cells.

(A) Quantification of GTTR fluorescence intensity in a control culture pre-treated with 1% DMSO before the addition of 0.2  $\mu$ M GTTR, compared to cultures pre-treated with 100  $\mu$ M carvedilol or **13**. Both compounds significantly reduced GTTR loading ( $p < 0.001$ ). No

1 significant difference in reduction was seen between the two compounds. (B-D) A representative  
2 fluorescence image from which intensity values were measured and a DIC image for: (B and B')  
3 the control (C and C') carvedilol and (D and D') **13**. Asterisks indicate the first row of OHCs,  
4 from which fluorescence intensity values were taken. N = 30 cells, with 10 cells analysed from 3  
5 separate experiments. Scale bar is 50  $\mu\text{m}$ .

## 6

### 7 **Comparison of protection and toxicity of carvedilol with compound **13** in zebrafish larvae**

8 In order to compare the protective effect of **13** to that of carvedilol *in vivo*, 4 day post  
9 fertilisation (dpf) zebrafish larvae were treated with either neomycin or gentamicin in the  
10 presence of each compound and the numbers of remaining hair cells were assessed  
11 (Supplemental Figure 1A-D). Dose-response curves for carvedilol and compound **13** were  
12 constructed and  $\text{EC}_{50}\text{s}$  were derived. The  $\text{EC}_{50}\text{s}$  for carvedilol and **13** protection against  
13 neomycin damage were 2.47  $\mu\text{M}$  and 2.08  $\mu\text{M}$  respectively. The  $\text{EC}_{50}$  for carvedilol protection  
14 against gentamicin damage was 10.95  $\mu\text{M}$ , whilst for compound **13** it was 10.81  $\mu\text{M}$ . The  
15 protective effect of these compounds therefore extends to other AGs in addition to gentamicin.

16 We then assessed the toxicity of carvedilol and compound **13** by treating 3 dpf zebrafish larvae  
17 with each at 30 and 100  $\mu\text{M}$  for 48 h (see Supplemental Methods). At a concentration of 100  $\mu\text{M}$   
18 carvedilol killed the larvae in two out of three trials, whilst it was not toxic at 30  $\mu\text{M}$ . With  
19 compound **13**, neither concentration was toxic for the larvae. Larvae treated with 100  $\mu\text{M}$   
20 carvedilol had slowed or no circulation, while those treated with 30  $\mu\text{M}$  of carvedilol or either  
21 concentration of compound **13** had no obvious defects in circulation. Treated larvae were startled  
22 and assayed for movement. As expected larvae treated with 100  $\mu\text{M}$  carvedilol showed reduced

1 movement, whilst those treated with 100  $\mu\text{M}$  of compound **13** showed increased movement  
2 compared to control.

### 3 4 **Assessing effects of carvedilol and compound 13 on the antimicrobial efficacy of** 5 **gentamicin.**

6 Carvedilol and compound **13** were tested in a bacterial cell viability assay to identify if either of  
7 these compounds decreased the antimicrobial activity of gentamicin. The Minimum Inhibitory  
8 Concentration (MIC) of gentamicin was established for three clinically important strains of  
9 bacteria: *Klebsiella pneumoniae*, *Pseudomonas aeruginosa* and *Staphylococcus aureus*. The  
10 bacteria were treated with gentamicin at 1x MIC (2.2  $\mu\text{M}$ ) together with 2.2  $\mu\text{M}$  or 11  $\mu\text{M}$   
11 carvedilol or compound **13** (1x or 5x the gentamicin MIC). Neither of the compounds resulted in  
12 an observable reduction in gentamicin antimicrobial activity (Supplemental Figure 2A-C).

### 13 14 **Discussion and conclusion**

15 The non-selective  $\alpha$ - and  $\beta$ -adrenergic blocker carvedilol was reported to provide protection  
16 against AG damage in a whole zebrafish larval model study.<sup>22</sup> Here we investigated its potential  
17 using in a mammalian system of AG-induced toxicity, mouse cochlear cultures, and zebrafish  
18 larvae. In parallel, we investigated its potential molecular target by studying its  
19 electrophysiological profile. Firstly, we determined that carvedilol (10 and 20  $\mu\text{M}$ ) was able to  
20 fully protect cochlear cultures against the damage caused by exposure to 5  $\mu\text{M}$  gentamicin for 48  
21 h. Unfortunately, carvedilol proved to be cytotoxic at higher concentrations ( $\geq 30$   $\mu\text{M}$ ) and



1 caused severe damage to the mechanosensory hair bundles when tested at 20  $\mu$ M, both alone and  
2  
3 together with gentamicin. Despite this, we decided to investigate further the mode of protection  
4  
5 of carvedilol by studying its potential interaction with the MET channel, which is the main entry  
6  
7 route of AGs into hair cells. From our experiments, carvedilol proved to be a relatively high-  
8  
9 affinity, permeant, and reversible blocker of the MET current with a  $K_D$  of 6.3  $\mu$ M at a  
10  
11 physiologically relevant potential of -164 mV. To fully evaluate its otoprotective profile, we  
12  
13 decided to investigate the structure activity relationship (SAR) of carvedilol aimed at improving  
14  
15 its affinity for the MET channel and its protective effect as well as reducing its cytotoxicity.  
16  
17  
18 From an initial investigation, we established that the carbazole moiety is needed for both  
19  
20 protection and interaction with the channel, with neither compound **2** nor **4** protecting hair cells  
21  
22 from gentamicin or blocking the MET current. Interestingly, the replacement of the anisole  
23  
24 moiety with a phenyl group as in compound **6** led to an increased cytotoxicity while still  
25  
26 providing the same level of block of the MET current as its parent derivative carvedilol. The  
27  
28 replacement of the anisole for an alkyl chain as in compound **7** led to a retention of its protective  
29  
30 effect and only slightly reduced its effect on the MET current. We then investigated the role of  
31  
32 the  $\beta$ -amino alcohol linker with regard to its interaction with the channel. The removal of the  
33  
34 hydroxyl group, compound **13**, resulted in an almost complete block of the MET current at 10  
35  
36  $\mu$ M and at least same protective effect against gentamicin damage compared to carvedilol. These  
37  
38 data show that the hydroxyl group is not needed for the interaction with the channel and we can  
39  
40 postulate that the enhanced block of the channel may be derived by an increased basicity of the  
41  
42 nitrogen, with a calculated pKa for compound **13** and carvedilol being 9.3 and 8.7 respectively,  
43  
44 which may lead to a stronger interaction with the channel. To our surprise, the extension of just  
45  
46 one extra carbon in the alkyl chain spacer between the carbazole and the basic centre, compound  
47  
48  
49  
50  
51  
52  
53  
54  
55  
56  
57  
58  
59  
60

**14**, proved to be detrimental as the compound was found to be more toxic than the parent compound. The role of the basic centre was investigated by substituting the nitrogen with a carbon (**15**) or by making the nitrogen non-basic (**19**). Neither of these compounds had any protective effect supporting the need for a basic centre that is positively charged at physiological pH for the protective effect. Also unsuccessful was the conversion of the secondary amine into a tertiary cyclic amine, as compound **8** did not have any protective effect against gentamicin damage. In compound **9** we inserted a second ethyl-anisole moiety and it was found to interact tightly with the channel and to act as a non-permeant blocker as noted by the lack of the release of the block at the extreme hyperpolarised (-164 mV) potential, probably due to some new interactions between the channel and the second anisole moiety. However, the level of the block of the MET current was reduced if compared to carvedilol and it was only partially protective. We then investigated two isomers of carvedilol moving the sidechain to the 2-position (**21**) or linking it to the nitrogen in the carbazole ring (**23**); both compounds were found to be toxic to the cochlear cultures. Driven by the results obtained with compounds **13** (improved protective effect and block of the MET current) and **9** (non-permeant MET channel blocker) we designed compound **16**, which lacks the hydroxyl group as in compound **13** and has the second ethyl-anisole as in compound **9**. Compound **16** proved to be only partially protective but we noticed a lack of consistency during the assays which is probably due to the poor solubility of this compound in the biological media preventing any meaningful interpretation of the results. Whilst we solved the solubility issue for this compound by substituting the second ethyl-anisole moiety with an ethyl morpholine **25** this did not translate into an increased protective effect. We then investigated other adrenergic and calcium blockers, with compounds **26**, **27** and **29** (propranolol, CGP20712 and verapamil respectively) not showing any protective effect, and **28** (naftopidil)

only offering partial protection at 20  $\mu\text{M}$ . Interestingly, **28** is the only compound that showed some protection but does not have the carbazole moiety and bears a naphthol ring. Based on our previous findings showing d-tubocurarine is a potent blocker of the MET channel current ( $K_D = 2.2 \mu\text{M}$ ) without showing any toxicity at higher concentration (50  $\mu\text{M}$ ),<sup>20</sup> the cytotoxic effect observed with some of these compounds is unlikely to be related to their ability to block the MET channel and is probably series related. A hit-to-lead optimisation campaign will be focussed on increasing the protective effect, reducing the toxicity, and addressing any adrenergic effect of these compounds. In addition, there will be the possibility of formulating the potential otoprotective agent to allow administration into the inner ear via transtympanic injection.

From a mechanistic point of view, we investigated in more detail the interaction of **13**, the most protective derivative, with the MET channel. This compound showed a very similar interaction with the channel to carvedilol, having a  $K_D$  of 4.6  $\mu\text{M}$  at a potential of -164 mV. Kinetics of MET channel block showed that both carvedilol and **13** are open channel blockers suggesting that they are able to interact with the channel only when it is open. As shown in the energy profiles graph, both carvedilol and **13** bind tighter to the negatively charged vestibule of the MET channel compared to the aminoglycoside DHS with a longer time consequently spent inside the channel. This result reflects on the rate of entry into the cells for these compounds, which is considerably lower (10 fold) compared to DHS. This stronger interaction with the MET channel may be behind the protective effect offered by carvedilol and **13** which hinders the interaction of aminoglycoside with the channel and as a consequence reducing its entry into the hair cells. The stronger protection of **13** ( $E_b$  -21.3 kT) compared to carvedilol may be due to it binding inside the channel pore more strongly than carvedilol ( $E_b$  -15.4 kT) (Figure 16). Both

carvedilol and compound **13** were able to block the loading of GTTR into the hair cells, further supporting the notion that the protective effect of both compounds is due to their block of the MET channel and the prevention of AG uptake into hair cells.

Finally, to exclude a protective effect specific to gentamicin, we compared the protection of carvedilol and compound **13** against neomycin using hair cells in the lateral line organs of zebrafish larvae. Both compounds were protective against neomycin damage at a concentration of  $\geq 12.5 \mu\text{M}$ , and found to be slightly less effective when tested against gentamicin, providing full protection at a concentration  $\geq 25 \mu\text{M}$ . In addition, neither carvedilol nor compound **13** interfered with gentamicin antimicrobial activity.

In conclusion, we established that carvedilol is able to protect cochlear cultures from AG-induced damage, although it is also cytotoxic *in vitro* at higher concentrations. We have established a clear SAR identifying the need for a carbazole moiety, a basic centre and preferentially an anisole moiety. The toxicity observed *in vitro* with cochlear cultures may not be an issue as carvedilol is widely used in the clinic and is not associated with hearing loss. Furthermore, carvedilol and its derivatives did not show a toxic effect *in vivo* with zebrafish larvae at  $30 \mu\text{M}$ . Although the ‘therapeutic window’ is narrow *in vitro*, our current data show carvedilol and its derivatives are a valid chemical starting point for the future development of drugs that will prevent AGs induced ototoxicity, and that the MET channel is a potential target for such compounds.

## Experimental Section

1 All commercial reagents were purchased from Sigma-Aldrich, Alfa Aesar, Apollo Scientific,  
2 Fluorochem or Tokyo Chemical Industry and of the highest available purity. Unless otherwise  
3 stated, chemicals were used as supplied without further purification. Anhydrous solvents were  
4 purchased from Acros (AcroSeal™) or Sigma-Aldrich (SureSeal™) and were stored under  
5 nitrogen. Petroleum ether refers to the fraction with a boiling point between 40 °C and 60 °C.  
6 Thin Layer Chromatography (TLC): pre-coated aluminium-backed plates (60 F254, 0.2 mm  
7 thickness, Merck) were visualized under both short- and long-wave UV light (254 and 366 nm).  
8 Flash column chromatography was carried out using commercial pre-packed columns from  
9 Biotage, Isco, Grace or filled with Merck silica gel 60 (40-63 µm) or C18 silica on an ISCO  
10 Combiflash Rf or a Biotage Isolera Prime. HPLC purification was performed on an Agilent 1100  
11 series HPLC spectrometer, using a Phenomenex Luna 10 µm C18 150 mm × 15 mm column,  
12 eluted using water and acetonitrile at 15 mL/min and detected at 254 nm.

13 Proton nuclear magnetic resonance spectra were recorded at 500 MHz or 600 MHz on a Varian  
14 VNMRS 500 MHz or Varian VNMRS 600 MHz spectrometers respectively (at 30 °C), using  
15 residual isotopic solvent ( $\text{CHCl}_3$ ,  $\delta = 7.27$  ppm, DMSO  $\delta = 2.50$  ppm) as an internal reference.  
16 Chemical shifts are quoted in parts per million (ppm). Coupling constants (J) are recorded in  
17 Hertz (Hz). The following abbreviations are used in the assignment of NMR signals: s (singlet),  
18 d (doublet), t (triplet), q (quartet), qn (quintet), m (multiplet), bs (broad singlet), dd (doublet of  
19 doublet), dt (doublet of triplet). Carbon nuclear magnetic resonance spectra were recorded at  
20 125 MHz or 151 MHz on a Varian 500 MHz or 600 MHz spectrometers respectively and are  
21 proton decoupled, using residual isotopic solvent ( $\text{CHCl}_3$ ,  $\delta = 77.00$  ppm, DMSO  $\delta = 39.52$  ppm)  
22 as an internal reference.

LCMS data was recorded on a Waters 2695 HPLC using a Waters 2487 UV detector and a Thermo LCQ ESI-MS. Samples were eluted through a Phenomenex Lunar 3  $\mu$ m C18 50 mm  $\times$  4.6 mm column, using water and acetonitrile acidified by 0.1% formic acid at 1 mL/min and detected at 254 nm. The following methods were used: method 1: water (+0.1% formic acid)/ acetonitrile (+0.1% formic acid) = from 65/35 to 10/90 in 3.5 min, then isocratic 10/90 0.4 min, then from 10/90 to 65/35 in 0.1 min; method 2: water (+0.1% formic acid)/ acetonitrile (+0.1% formic acid) = from 70/30 to 10/90 in 5 min, then isocratic 10/90 1.0 min, then from 10/90 to 70/30 in 0.5 min and then isocratic 70/30 for 0.5 min.

LCMS (MDAP): LCMS data was recorded on a Shimatzu Prominence Series coupled to a LCMS-2020 ESI and APCI mass spectrometer. Samples were eluted through a Phenomenex Gemini 5 $\mu$  C18 110A 250 mm  $\times$  4.6 mm column, using water and acetonitrile acidified by 0.1% formic acid at 1 mL/min and detected at 254 nm. The following method, marked as method 3, was used: water (+0.1% formic acid)/ acetonitrile (+0.1% formic acid) = isocratic 95/5 1 min, then from 95/5 to 5/95 in 20 min, then isocratic 5/95 for 4 min, then from 5/95 to 70/30 in 5 min.

Physicochemical properties were calculated using MarvinSketch 16.8.15.0 by ChemAxon (<https://www.chemaxon.com>).

Compound purity was assured by a combination of high field multinuclear NMR (<sup>1</sup>H, <sup>13</sup>C) and HPLC; purity by the later was always >95%.

## Chemistry

**Synthesis of 2-((2-methoxyphenoxy)methyl)oxirane (1).** A mixture of 2-methoxyphenol (1.0 g, 8.06 mmol), 2-(bromomethyl)oxirane (0.69 mL, 8.06 mmol) and anhydrous K<sub>2</sub>CO<sub>3</sub> (2.23 g, 16.11 mmol) in DMF (5 mL) was stirred at 70 °C for 6 h. After cooling, the solvent was

1 evaporated under reduced pressure and the residue was dissolved in water and the aqueous phase  
2 was extracted with ethyl acetate. The organic phase was washed with saturated NaHCO<sub>3</sub>  
3 solution, dried over MgSO<sub>4</sub>, filtered and concentrated. The residue was then purified by flash  
4 column chromatography gradient elution of petroleum ether/ethyl acetate (100/0 to 0/100) to  
5 give **1** as an oil which crystallised to give a colourless solid (0.90 g, 62%). <sup>1</sup>H NMR (DMSO 600  
6 MHz): δ 6.95 (td, J = 7.6, 1.6 Hz, 2H), 6.90 (td, J = 7.7, 1.6 Hz, 1H), 6.85 (td, J = 7.6, 1.6 Hz,  
7 1H), 4.25 (dd, J = 11.3, 2.8 Hz, 1H), 3.78 (dd, J = 11.3, 6.6 Hz, 1H), 3.74 (s, 3H), 3.30 (d, J = 2.6  
8 Hz, 1H), 2.81 (dd, J = 5.1, 4.2 Hz, 1H), 2.67 (dd, J = 5.1, 2.7 Hz, 1H).

#### 9 **Synthesis of 1-(2-methoxyphenoxy)-3-[2-(2-methoxyphenoxy)ethylamino]propan-2-ol (2)** A

10 solution of 2-(2-methoxyphenoxy)ethanamine (0.84 mL, 5.55 mmol) in ethylene glycol dimethyl  
11 ether (1 mL) was heated to 80 °C. Then, a solution of **1** (0.25 g, 1.39 mmol) in ethylene glycol  
12 dimethyl ether (1 mL) was added dropwise and the reaction mixture was stirred at 80 °C for 5 h.  
13 Then, **1** (0.12 g, 0.67 mmol) in ethylene glycol dimethyl ether (0.50 mL) was added dropwise  
14 and the reaction mixture was stirred at 80 °C for further 1 h. After cooling, the solvent was  
15 evaporated under reduced pressure and the residue was purified by flash column chromatography  
16 gradient elution of petroleum ether/ethyl acetate (100/0 to 0/100). The compound was further by  
17 HPLC gradient elution of water/acetonitrile = 95:5 to 0:100 in 20 min to give **2** as a colourless  
18 solid (0.12 g, 25%). <sup>1</sup>H NMR (DMSO 500 MHz): δ 6.96-6.94 (m, 4H), 6.89-6.85 (m, 4H), 4.95  
19 (s, 1H), 3.99 (t, J = 5.6 Hz, 2H), 3.93-3.83 (m, 3H), 3.73 (d, J = 3.2 Hz, 6H), 2.88 (t, J = 5.6 Hz,  
20 2H), 2.80-2.71 (m, 1H), 2.68-2.60 (m, 1H). <sup>13</sup>C NMR (DMSO 126 MHz): δ 149.78, 149.71,  
21 148.83, 148.66, 121.55, 121.45, 121.25, 121.23, 114.40, 114.26, 113.01, 112.93, 72.13, 69.08,  
22 68.78, 56.07, 53.03, 48.98. LCMS: method 2: RT: 0.71 min; M+H<sup>+</sup>: 348.38. LCMS: Method 3,  
23 RT = 11.22 min; M+H<sup>+</sup>: 348.40.

**Synthesis of 1-(2-bromoethoxy)-2-methoxy-benzene (3).** A solution of 2-methoxyphenol (4.0 mL, 36.38 mmol) and NaOH (4.37 g, 109.13 mmol) in water (25 mL) was added dropwise to 1,2-dibromoethane (25.08 mL, 291.03 mmol) and the reaction mixture was then stirred at reflux for 3 h. After cooling, the phases were separated and the organic phase was concentrated. The residue was purified by flash column chromatography gradient elution of petroleum ether/ethyl acetate (100/0 to 50/50) to give a yellow oil which crystallised at room temperature to give **3** as a yellow solid (1.84 g, 22%). <sup>1</sup>H NMR (DMSO 500 MHz): δ 7.00-6.95 (m, 2H), 6.95-6.91 (m, 1H), 6.89-6.84 (m, 1H), 4.27 (t, J = 5.5 Hz, 2H), 3.80-3.73 (m, 5H).

**Synthesis of 2-(2-methoxyphenoxy)-N-[2-(2-methoxyphenoxy)ethyl]ethanamine (4).** 2-(2-methoxyphenoxy)ethanamine (0.90 mL, 5.98 mmol) and TEA (1.67 mL, 11.96 mmol) were added to a solution of **3** (1.38 g, 5.98 mmol) in THF (10 mL) and the reaction mixture was stirred at 65 °C for 5 h. Then, TEA (0.83 mL, 5.98 mmol) was added and the reaction mixture was stirred at 65 °C for further 1 h. After cooling, the solvent was removed under reduced pressure, and the residue was triturated with water and ethyl acetate. The precipitate was filtered to give a first crop of the desired compound as a colourless solid (0.52 g, 26%). The layers were then separated and the aqueous phase was extracted with ethyl acetate. The combined organic phase was washed with brine, dried over MgSO<sub>4</sub>, filtered and concentrated to give **4** as a yellow oil which crystallised at room temperature. The solid was washed four times with a mixture water/ethyl acetate (5/1) to give a second crop of the desired compound **4** as an off-white solid (0.28 g, 14%). <sup>1</sup>H NMR (DMSO 600 MHz): δ 6.96-6.93 (m, 4H), 6.89-6.82 (m, 4H), 4.00 (t, J = 5.6 Hz, 4H), 3.72 (s, 6H), 2.93 (t, J = 5.6 Hz, 4H). <sup>13</sup>C NMR (DMSO 151 MHz): δ 149.64, 148.49, 121.52, 121.16, 114.16, 112.66, 68.93, 55.88, 48.67. LCMS: Method 2: RT: 0.68 min; M+H<sup>+</sup>: 318.12. LCMS: Method 3, RT = 11.37; M+H<sup>+</sup>: 318.35.



**Synthesis of 4-(oxiran-2-ylmethoxy)-9H-carbazole (5).** To a solution of NaOH (0.48 g, 12.01 mmol) in water (10 mL), 9H-carbazol-4-ol (2.0 g, 10.92 mmol) and DMSO (5 mL) were added followed by dropwise addition of 2-(bromomethyl)oxirane (1.4 mL, 16.37 mmol). The reaction mixture was then heated at 45 °C for 16 h. After cooling, water (20 mL) was added and the reaction mixture was stirred at room temperature for 1 h. The precipitate formed was filtered and the wet solid was recrystallised from isopropanol to give **5** as a brown solid (0.82 g, 31%). A second crop of **5** was also obtained as a brown solid (0.63 g, 24%). <sup>1</sup>H NMR (DMSO 600 MHz): δ 11.26 (s, 1H), 8.15 (d, J = 7.8 Hz, 1H), 7.44 (d, J = 8.0 Hz, 1H), 7.33 (dt, J = 8.2, 7.1 Hz, 1H), 7.28 (t, J = 8.0 Hz, 1H), 7.17-7.11 (m, 1H), 7.08 (d, J = 8.0 Hz, 1H), 6.68 (d, J = 7.9 Hz, 1H), 4.54 (dd, J = 11.2, 2.6 Hz, 1H), 4.08 (dd, J = 11.2, 6.2 Hz, 1H), 3.52 (ddd, J = 6.5, 4.4, 2.5 Hz, 1H), 2.92 (t, J = 4.7 Hz, 1H), 2.83 (dd, J = 5.1, 2.7 Hz, 1H). <sup>13</sup>C NMR (DMSO 151 MHz): δ 154.93, 141.56, 139.39, 126.89, 125.10, 122.72, 122.00, 119.09, 111.93, 110.91, 104.68, 101.14, 69.21, 50.38, 44.26. LCMS: Method 2: RT: 3.65 min; M+H<sup>+</sup>: 240.16.

**Synthesis of 1-(9H-carbazol-4-yloxy)-3-(2-phenoxyethylamino)propan-2-ol (6).** A solution of 2-phenoxyethanamine (0.22 mL, 1.67 mmol) in ethylene glycol dimethyl ether (0.75 mL) was heated at 80 °C then a solution of **5** (0.10 g, 0.42 mmol) in ethylene glycol dimethyl ether (0.75 mL) was added dropwise and the reaction mixture was stirred at 80 °C for 24 h. After cooling, the solvent was removed under reduced pressure and the residue was purified by flash column chromatography gradient elution of petroleum ether/ethyl acetate (100/0 to 0/100) to give the desired compound which was further by reverse phase HPLC gradient elution of water/acetonitrile = 95:5 to 0:100 in 20 min to give **6** as an off-white solid (0.085 g, 54%). <sup>1</sup>H NMR (DMSO 600 MHz): δ 11.21 (s, 1H), 8.20 (d, J = 7.8 Hz, 1H), 7.42 (d, J = 8.0 Hz, 1H), 7.34-7.28 (m, 1H), 7.28-7.21 (m, 3H), 7.10 (t, J = 7.4 Hz, 1H), 7.05 (d, J = 8.0 Hz, 1H), 6.89 (dd,

1 J = 7.9, 6.3 Hz, 3H), 6.66 (d, J = 7.9 Hz, 1H), 5.13 (d, J = 4.9 Hz, 1H), 4.19-4.11 (m, 2H), 4.11-  
2 4.06 (m, 1H), 4.01 (t, J = 5.6, 2H), 2.93 (td, J = 5.5, 2H), 2.81 (dd, J = 11.9, 6.8 Hz, 1H), 2.01 (s,  
3 1H). <sup>13</sup>C NMR (DMSO 151 MHz): δ 159.02, 155.40, 141.53, 139.34, 129.88, 126.92, 124.94,  
4 122.90, 122.17, 119.00, 114.86, 112.00, 110.77, 104.25, 100.87, 70.89, 68.91, 67.86, 53.08,  
5 48.90. LCMS: Method 2: RT: 1.53 min; M+H<sup>+</sup>: 377.19.

6 **Synthesis of 1-(butylamino)-3-(9H-carbazol-4-yloxy)propan-2-ol (7).** A solution of butan-1-  
7 amine (0.50 mL, 5.02 mmol) in ethylene glycol dimethyl ether (0.75 mL) was heated at 80 °C in  
8 a sealed tube. Then, a solution of **5** (0.12 g, 0.50 mmol) in ethylene glycol dimethyl ether (0.75  
9 mL) was added dropwise and the reaction mixture was stirred at 80 °C for 2.5 h. After cooling,  
10 the solvent was removed under reduced pressure and the residue was left overnight, continuing  
11 the reaction with no solvent. The residue was then purified by flash column chromatography  
12 gradient elution of petroleum ether/ethyl acetate (100/0 to 0/100) to give the desired compound  
13 as a yellow gum, which was further purified by reverse phase HPLC gradient elution of  
14 water/acetonitrile = 95/5 to 0/100 in 20 min to give **7** as a pale yellow solid (0.055 g, 35%). <sup>1</sup>H  
15 NMR (DMSO 500 MHz): δ 11.21 (s, 1H), 8.21 (d, J = 7.7 Hz, 1H), 7.43 (d, J = 8.0 Hz, 1H),  
16 7.35-7.30 (m, 1H), 7.28 (t, J = 8.0 Hz, 1H), 7.12 (t, J = 7.4 Hz, 1H), 7.06 (d, J = 8.0 Hz, 1H),  
17 6.67 (d, J = 7.9 Hz, 1H), 5.04 (bs, 1H), 4.18-4.11 (m, 2H), 4.09-4.04 (m, 1H), 2.83 (dd, J = 11.9,  
18 4.8 Hz, 1H), 2.73 (dd, J = 11.9, 6.8 Hz, 1H), 2.55 (dt, J = 6.9, 2.8 Hz, 2H), 1.47-1.35 (m, 2H),  
19 1.35-1.25 (m, 2H), 0.85 (t, J = 7.3 Hz, 3H). <sup>13</sup>C NMR (DMSO 126 MHz): δ 155.47, 141.59,  
20 139.40, 126.90, 124.94, 122.90, 122.23, 118.94, 110.78, 109.99, 104.25, 100.95, 71.05, 68.84,  
21 53.19, 49.61, 32.28, 20.39, 14.36. LCMS: Method 2: RT: 0.69 min; M+H<sup>+</sup>: 313.02. LCMS:  
22 Method 3, RT = 11.65; M+H<sup>+</sup>: 313.35.

**Synthesis of 1-(9H-carbazol-4-yloxy)-3-(4-phenylpiperazin-1-yl)propan-2-ol (8).** A mixture of **5** (0.20 g, 0.84 mmol) and phenyl piperazine (0.13 mL, 0.84 mmol) in ethanol (25 mL) was stirred at 65 °C for 16 h. The reaction solvent was then removed under reduced pressure and the residue was purified flash column chromatography gradient elution of petroleum ether/ethyl acetate (100/0 to 0/100) to give **8** as a colourless oil which crystallised on standing (0.28 g, 80%). <sup>1</sup>H NMR (CDCl<sub>3</sub> 500 MHz): δ 8.29 (d, J = 7.8 Hz, 1H), 8.09 (s, 1H), 7.44-7.37 (m, 1H), 7.37-7.21 (m, 5H), 7.06 (d, J = 8.1 Hz, 1H), 6.95 (d, J = 8.1, 2H), 6.88 (t, J = 7.3 Hz, 1H), 6.69 (d, J = 8.0 Hz, 1H), 4.42-4.29 (m, 2H), 4.28-4.23 (m, 1H), 3.32-3.19 (m, 5H), 2.95-2.87 (m, 1H), 2.87-2.75 (m, 2H), 2.73-2.65 (m, 2H). <sup>13</sup>C NMR (CDCl<sub>3</sub> 126 MHz): δ 151.17, 150.82, 144.11, 138.69, 129.13, 126.66, 125.01, 122.93, 119.88, 119.67, 117.73, 116.15, 110.01, 103.82, 101.21, 70.28, 65.85, 61.07, 53.46, 53.31, 49.30. LCMS: Method 3, RT = 12.39; M+H<sup>+</sup>: 402.25.

**Synthesis of 1-[bis[2-(2-methoxyphenoxy)ethyl]amino]-3-(9H-carbazol-4-yloxy)propan-2-ol (9).** A solution of **4** (0.13 g, 0.42 mmol) in ethylene glycol dimethyl ether (0.50 mL) was heated in a sealed tube at 80 °C. A solution of **5** (0.10 g, 0.42 mmol) in ethylene glycol dimethyl ether (0.50 mL) was added dropwise and the reaction was heated at 80 °C for 5 h. Then, **4** (0.13 g, 0.42 mmol) was added and the reaction mixture was stirred at 80 °C for 24 h. Then, a solution of **4** (0.07 g, 0.21 mmol) in ethylene glycol dimethyl ether (0.50 mL) was added and the reaction mixture was stirred at 80 °C for further 18 h. After cooling, the solvent was removed under reduced pressure and the residue was purified by flash column chromatography gradient elution of petroleum ether/ethyl acetate (100/0 to 0/100) to give the desired compound which was further purified by flash column chromatography gradient elution of petroleum ether/ethyl acetate (100/0 to 20/100) to give the desired compound as a yellow oil which was triturated with methanol/acetone to give **9** a colourless solid (0.12 g, 52%). <sup>1</sup>H NMR (DMSO 600 MHz): δ

1 11.20 (s, 1H), 8.22 (d, J = 7.7 Hz, 1H), 7.40 (d, J = 8.1 Hz, 1H), 7.31-7.25 (m, 1H), 7.22 (t, J =  
2 8.0 Hz, 1H), 7.09-7.00 (m, 2H), 6.88 (d, J = 8.0 Hz, 2H), 6.84-6.80 (m, 2H), 6.75-6.69 (m, 4H),  
3 6.58 (d, J = 7.9 Hz, 1H), 4.92 (d, J = 4.6 Hz, 1H), 4.23-4.15 (m, 2H), 4.14-4.07 (m, 1H), 4.00-  
4 3.95 (m, 4H), 3.65 (s, 6H), 3.05-2.96 (m, 5H), 2.83 (dd, J = 13.3, 6.0 Hz, 1H). <sup>13</sup>C NMR (DMSO  
5 151 MHz): δ 155.47, 149.41, 148.45, 141.53, 139.33, 126.91, 124.88, 122.90, 122.22, 121.17,  
6 121.07, 118.96, 113.45, 112.58, 111.99, 110.73, 104.13, 100.65, 70.37, 68.42, 67.42, 58.54,  
7 55.86, 54.74. LCMS: Method 2: RT: 2.37 min; M+H<sup>+</sup>: 557.40. LCMS: Method 3, RT = 14.04  
8 min; M+H<sup>+</sup>: 557.60.

9 **Synthesis of 4-(3-bromopropoxy)-9H-carbazole (10).** A solution of 4-hydroxycarbazole (0.50  
10 g, 2.73 mmol), 1,3-dibromopropane (0.83 mL, 8.19 mmol) and KOH (0.15 g, 2.73 mmol) in  
11 acetonitrile (25 mL) was stirred at room temperature overnight. After this period, 1,3-  
12 dibromopropane (0.42 mL, 4.09 mmol) and KOH (0.046 g, 0.82 mmol) were added and the  
13 stirring was continued for further 3 h. The solvent was then removed under reduced pressure and  
14 the residue was purified by flash column chromatography gradient elution of petroleum  
15 ether/ethyl acetate (100/0 to 50/50) to give **10** as a colourless solid (0.50 g, 59%). <sup>1</sup>H NMR  
16 (CDCl<sub>3</sub>, 500 MHz): δ 8.25 (d, J = 7.8 Hz, 1H), 8.07 (s, 1H), 7.46-7.37 (m, 2H), 7.36-7.30 (m,  
17 1H), 7.26-7.22 (m, 1H), 7.07 (d, J = 8.1 Hz, 1H), 6.71 (d, J = 8.0 Hz, 1H), 4.41 (t, J = 5.8 Hz,  
18 2H), 3.78 (t, J = 6.5 Hz, 2H), 2.55 (p, J = 6.2 Hz, 2H). LCMS: Method 1: RT: 3.67 min; M+H<sup>+</sup>:  
19 304.06, 306.05.

20 **Synthesis of 4-(4-bromobutoxy)-9H-carbazole (11).** A mixture of 4-hydroxycarbazole (0.50 g,  
21 2.73 mmol), 1,4-dibromobutane (0.89 mL, 8.19 mmol) and KOH (0.15 g, 2.73 mmol) in  
22 acetonitrile (25 mL) was stirred at room temperature for 16 h. The solvent was removed under  
23 reduced pressure and the residue was purified by flash column chromatography gradient elution

of petroleum ether/ethyl acetate (100/0 to 50/50) to give **11** as a colourless solid (0.47 g, 52%).  
<sup>1</sup>H NMR (CDCl<sub>3</sub> 500 MHz): δ 8.28 (d, J = 7.8 Hz, 1H), 8.05 (s, 1H), 7.43-7.36 (m, 2H), 7.32 (t, J = 8.0 Hz, 1H), 7.27-7.22 (m, 1H), 7.04 (d, J = 8.1 Hz, 1H), 6.66 (d, J = 8.0 Hz, 1H), 4.27 (t, J = 5.8 Hz, 2H), 3.58 (t, J = 6.4 Hz, 2H), 2.27-2.21 (m, 2H), 2.20-2.13 (m, 2H). <sup>13</sup>C NMR (CDCl<sub>3</sub> 126 MHz): δ 138.65, 137.28, 126.65, 124.93, 122.93, 119.65, 117.73, 109.94, 103.49, 100.97, 88.29, 88.28, 66.76, 33.64, 29.61, 28.00. LCMS: Method 1: RT: 3.84 min; M+H<sup>+</sup>: 318.03, 319.95.

**Synthesis of 4-(6-bromohexoxy)-9H-carbazole (12).** A solution of 4-hydroxy carbazole (0.50 g, 2.73 mmol), 1,6-dibromohexane (1.26 mL, 8.19 mmol) and KOH (0.31 g, 5.46 mmol) in acetonitrile (25 mL) was stirred at room temperature for 5 h. Then, the solvent was removed under reduced pressure and the residue was purified by flash column chromatography gradient elution of petroleum ether/ethyl acetate (100:0 to 0:100) to give **12** as a pale yellow solid (0.48 g, 51%). <sup>1</sup>H NMR (DMSO 600 MHz): 11.21 (s, 1H), 8.13 (dd, J = 7.8, 1.2 Hz, 1H), 7.43 (dt, J = 8.2, 0.9 Hz, 1H), 7.31 (ddd, J = 8.1, 7.1, 1.2 Hz, 1H), 7.26 (t, J = 8.0 Hz, 1H), 7.13 (ddd, J = 7.9, 7.2, 1.0 Hz, 1H), 7.04 (d, J = 8.0 Hz, 1H), 6.65 (d, J = 7.9 Hz, 1H), 4.17 (t, J = 6.3 Hz, 2H), 3.53 (t, J = 6.7 Hz, 2H), 1.91-1.82 (m, 4H), 1.63-1.45 (m, 4H). LCMS: Method 2: RT: 6.00 min; M+H<sup>+</sup>: 346.10, 348.06. Another fraction was isolated to give the bis-alkylated product as a yellow solid (0.20 g, 14%).

**Synthesis of 3-(9H-carbazol-4-yloxy)-N-[2-(2-methoxyphenoxy)ethyl]propan-1-amine (13).**

A solution of **10** (0.10 g, 0.33 mmol), 2-(2-methoxyphenoxy)ethanamine (0.15 mL, 0.99 mmol) and anhydrous K<sub>2</sub>CO<sub>3</sub> (0.14 g, 0.99 mmol) in anhydrous DMF (5 mL) was stirred at room temperature under a nitrogen atmosphere overnight. The solvent was then removed under reduced pressure and the residue was dissolved in DCM. The organic phase was washed with

water (5 times), dried over  $\text{MgSO}_4$ , filtered and concentrated. The residue was purified by flash column chromatography gradient elution of petroleum ether/ethyl acetate (100/0 to 0/100). The compound obtained was then further purified by HPLC gradient elution of water/acetonitrile = 95/5 to 0/100 in 20 min to give **13** as an off-white solid (0.025 g, 19%).  $^1\text{H}$  NMR (DMSO 600 MHz):  $\delta$  11.21 (s, 1H), 8.13 (d,  $J = 7.8$  Hz, 1H), 7.42 (d,  $J = 8.0$  Hz, 1H), 7.30 (ddd,  $J = 8.2, 7.1, 1.2$  Hz, 1H), 7.26 (t,  $J = 8.0$  Hz, 1H), 7.14 – 7.07 (m, 1H), 7.04 (d,  $J = 8.0$  Hz, 1H), 6.93-6.90 (m, 2H), 6.86 (td,  $J = 7.7, 1.7$  Hz, 1H), 6.82 (td,  $J = 7.6, 1.6$  Hz, 1H), 6.67 (d,  $J = 7.9$  Hz, 1H), 4.25 (t,  $J = 6.1$  Hz, 2H), 3.98 (t,  $J = 5.8$  Hz, 2H), 3.70 (s, 3H), 2.93 – 2.82 (m, 4H), 2.04 (p,  $J = 6.5$  Hz, 2H).  $^{13}\text{C}$  NMR (DMSO 151 MHz):  $\delta$  155.44, 149.64, 148.51, 141.51, 139.34, 126.94, 124.91, 122.56, 122.20, 121.46, 121.15, 119.03, 114.15, 112.66, 111.89, 110.83, 104.15, 100.85, 68.83, 66.14, 55.88, 48.77, 46.61, 30.04. LCMS: Method 2: RT: 1.77 min;  $\text{M}+\text{H}^+$ : 391.25; LCMS: Method 3, RT = 12.64;  $\text{M}+\text{H}^+$ : 391.45.

### Synthesis of 4-(9H-carbazol-4-yloxy)-N-[2-(2-methoxyphenoxy)ethyl]butan-1-amine (**14**).

To a solution of **11** (0.25 g, 0.79 mmol) in THF (20 mL) was added TEA (0.24 mL, 1.74 mmol) and 2-(2-methoxyphenoxy)ethanamine (0.13 g, 0.79 mmol) and the reaction was stirred at 65 °C for 4 h. The reaction mixture was cooled to room temperature and 2-(2-methoxyphenoxy)ethanamine (0.13 g, 0.79 mmol) and TEA (0.16 mL, 1.18 mmol) were added. The reaction mixture was reheated to 65 °C and stirred for further 20 h. After cooling, the solvent was removed under reduced pressure and the residue was purified by flash column chromatography gradient elution of petroleum ether/ethyl acetate (100/0 to 0/100) to give **14** as a colourless oil (0.11 g, 32%).  $^1\text{H}$  NMR ( $\text{CDCl}_3$  500 MHz):  $\delta$  8.31 (d,  $J = 7.6$  Hz, 2H), 7.41-7.33 (m, 2H), 7.31 (t,  $J = 8.0$  Hz, 1H), 7.25-7.20 (m, 1H), 7.02 (d,  $J = 8.1$  Hz, 1H), 6.97-6.86 (m, 4H), 6.64 (d,  $J = 8.0$  Hz, 1H), 4.21 (t,  $J = 6.5$  Hz, 2H), 4.14 (t,  $J = 5.2$  Hz, 2H), 3.84 (s, 3H), 3.05 (t,  $J$

1 = 5.3 Hz, 2H), 2.76 (t, J = 7.3 Hz, 2H), 2.10-1.92 (m, 2H), 1.83-1.72 (m, 3H). <sup>13</sup>C NMR (CDCl<sub>3</sub>, 126 MHz): δ 155.60, 140.94, 138.70, 126.63, 124.82, 123.03, 122.72, 121.47, 120.90, 119.54, 114.01, 112.61, 111.79, 109.98, 109.89, 103.31, 100.95, 88.27, 68.77, 67.74, 55.78, 49.56, 48.83, 27.31, 26.82. LCMS: Method 3, RT = 12.74; M+H<sup>+</sup>: 405.20.

**Synthesis of 4-[6-(2-methoxyphenoxy)hexoxy]-9H-carbazole (15).** A solution of **12** (0.10 g, 0.29 mmol), 2-methoxyphenol (0.06 mL, 0.58 mmol) and KOH (0.03 g, 0.58 mmol) in acetonitrile (8 mL) was stirred at room temperature for 6 h. Then, 2-methoxyphenol (0.06 mL, 0.58 mmol) and KOH (0.03 g, 0.58 mmol) were added and the stirring was continued for further 60 h. After this period, the solvent was removed under reduced pressure and the residue was purified by flash column chromatography gradient elution of petroleum ether/ethyl acetate (100:0 to 60:40) to give the desired compound which was washed with methanol to give **15** as an off-white solid (0.045 g, 40%). <sup>1</sup>H NMR (DMSO 600 MHz): δ 11.21 (s, 1H), 8.12 (d, J = 7.8 Hz, 1H), 7.42 (d, J = 8.0 Hz, 1H), 7.32-7.28 (m, 1H), 7.26 (t, J = 8.0 Hz, 1H), 7.09 (t, J = 7.5 Hz, 1H), 7.04 (d, J = 8.0 Hz, 1H), 6.91 (td, J = 7.7, 1.8 Hz, 2H), 6.87-6.80 (m, 2H), 6.66 (d, J = 7.9 Hz, 1H), 4.19 (t, J = 6.3 Hz, 2H), 3.94 (t, J = 6.5 Hz, 2H), 3.71 (s, 3H), 1.92 (p, J = 6.6 Hz, 2H), 1.76 (p, J = 6.8 Hz, 2H), 1.63 (p, J = 7.5 Hz, 2H), 1.55 (q, J = 7.8 Hz, 2H). <sup>13</sup>C NMR (DMSO 600 MHz): δ 155.45, 149.54, 148.66, 141.52, 139.34, 126.94, 124.91, 122.52, 122.20, 121.20, 121.16, 119.03, 113.74, 112.69, 111.89, 110.83, 104.15, 100.84, 68.53, 67.71, 55.92, 40.24, 29.30, 29.22, 25.94, 25.74. LCMS: Method 2: RT: 5.96 min; M+H<sup>+</sup>: 390.10.

**Synthesis of 3-(9H-carbazol-4-yloxy)-N,N-bis[2-(2-methoxyphenoxy)ethyl]propan-1-amine (16).** A solution of **4** (0.32 g, 0.97 mmol), **10** (0.10 g, 0.32 mmol) and K<sub>2</sub>CO<sub>3</sub> (0.13 g, 0.97 mmol) in anhydrous DMF (5 mL) was stirred at room temperature under a nitrogen atmosphere for 36 h. The solvent was then removed under reduced pressure and the residue was purified by

three sequential flash column chromatography: first column, gradient elution of DCM/methanol = 90/10; second column, gradient elution of DCM/methanol = (100/0 to 99/1); third column, gradient elution of petroleum ether/ethyl acetate (100/0 to 0/100) to give **16** as a colourless solid (4.8 mg, 3%). <sup>1</sup>H NMR (CDCl<sub>3</sub> 500 MHz): δ 8.29 (d, J = 7.8 Hz, 1H), 8.07 (s, 1H), 7.47 – 7.33 (m, 2H), 7.30 (t, J = 8.0 Hz, 1H), 7.18 (t, J = 7.4 Hz, 1H), 7.03 (d, J = 8.1 Hz, 1H), 6.92 – 6.83 (m, 5H), 6.83 – 6.73 (m, 4H), 6.65 (d, J = 8.0 Hz, 1H), 4.32 (t, J = 6.0 Hz, 2H), 4.16 – 4.09 (m, 4H), 3.80 (s, 5H), 3.12 (t, J = 6.4 Hz, 4H), 3.03 (t, J = 6.9 Hz, 2H), 2.20 (p, J = 6.5 Hz, 2H). <sup>13</sup>C NMR (CDCl<sub>3</sub> 126 MHz): δ 159.00, 155.63, 151.71, 146.04, 136.37, 129.83, 126.69, 124.81, 122.91, 120.96, 120.82, 119.65, 113.17, 111.74, 109.98, 109.86, 103.25, 100.88, 67.43, 65.68, 55.81, 53.88. LCMS: Method 3, RT = 14.01; M+H<sup>+</sup>: 541.30.

**Synthesis of ethyl 2-(9H-carbazol-4-yloxy)acetate (17).** A mixture of 4-hydroxycarbazole (1.90 g, 10.38 mmol), ethyl chloroacetate (1.11 mL, 10.38 mmol) and K<sub>2</sub>CO<sub>3</sub> (1.43 g, 10.38 mmol) in acetone (150 mL) were stirred at 56 °C for 16 h. The solvent was removed under reduced pressure and the residue was used in the next step with no further purification.

**Synthesis of 2-(9H-carbazol-4-yloxy)acetic acid (18).** A solution of **17** (0.72 g, 2.67 mmol) in THF (25 mL) was stirred with 1M aqueous NaOH (20 mL, 20 mmol) at room temperature for 16 h. The reaction mixture was then acidified with 1M HCl, and the organic layer was separated and concentrated under reduced pressure. The residue was triturated with ethyl acetate to give **18** as a colourless solid (0.16 g, 23%) and used in the next step with no further purification. <sup>1</sup>H NMR (DMSO 500 MHz): δ 11.27 (s, 1H), 8.24 (d, J = 7.8 Hz, 1H), 7.43 (d, J = 8.1 Hz, 1H), 7.32 (t, J = 7.6 Hz, 1H), 7.26 (t, J = 8.0 Hz, 1H), 7.13 (t, J = 7.5 Hz, 1H), 7.07 (d, J = 8.0 Hz, 1H), 6.57 (d, J = 8.0 Hz, 1H), 4.87 (s, 2H). LCMS: Method 2: RT: 0.52 min; M+H<sup>+</sup>: 242.03.



**Synthesis of 2-(9H-carbazol-4-yloxy)-N-[2-(2-methoxyphenoxy)ethyl]acetamide (19).** To a solution of **18** (0.075 g, 0.29 mmol), 2-(2-methoxyphenoxy)ethanamine (0.05 g, 0.29 mmol) and HOBt (0.054 g, 0.35 mmol) in anhydrous DMF (2 mL), EDC hydrochloride (0.068 g, 0.35 mmol) and DIPEA (0.15 mL, 0.88 mmol) were added and the reaction was stirred at room temperature for 16 h. After this period, the solvent was removed under reduced pressure and the residue was purified by flash column chromatography gradient elution of petroleum ether/ethyl acetate (90/10 to 0/100) to give **19** as a colourless solid (0.08 g, 64%). <sup>1</sup>H NMR (CDCl<sub>3</sub>, 500 MHz): δ 8.22 (d, J = 7.8 Hz, 1H), 8.17 (bs, 1H), 7.51 – 7.38 (m, 2H), 7.34 (d, J = 7.5 Hz, 1H), 7.29 (t, J = 8.0 Hz, 1H), 7.10 (d, J = 8.1 Hz, 1H), 7.00 (t, J = 7.5 Hz, 1H), 6.97-6.92 (m, 1H), 6.91-6.84 (m, 1H), 6.78 (d, J = 7.9 Hz, 1H), 6.63 (d, J = 8.0 Hz, 1H), 4.81 (s, 2H), 4.15 (t, J = 5.1 Hz, 2H), 3.81 (q, J = 5.4 Hz, 2H), 3.50 (s, 3H). <sup>13</sup>C NMR (CDCl<sub>3</sub>, 126 MHz): δ 168.85, 153.62, 141.03, 138.72, 131.74, 126.68, 125.27, 122.77, 122.32, 120.82, 119.88, 115.40, 111.89, 110.10, 104.89, 101.76, 68.64, 67.85, 55.42, 38.75. LCMS: Method 3, RT = 19.52; M+H<sup>+</sup>: 391.20.

**Synthesis of 2-(oxiran-2-ylmethoxy)-9H-carbazole (20).** To a solution of 2-hydroxycarbazole (1.0 g, 5.46 mmol), NaOH (0.24 g, 6.0 mmol) in water (5 mL) a solution of 2-(bromomethyl)oxirane (0.70 mL, 8.19 mmol) in DMSO (1 mL) was added dropwise. The reaction mixture was stirred at 45 °C for 16 h. After cooling to room temperature, the resulting precipitate was filtered and triturated with isopropanol to give the desired compound **20** as a colourless solid (0.13 g, 9%). <sup>1</sup>H NMR (CDCl<sub>3</sub>, 500 MHz): δ 8.02-7.90 (m, 3H), 7.41-7.31 (m, 2H), 7.21 (t, J = 7.4 Hz, 1H), 6.94 (s, 1H), 6.87 (d, J = 8.5 Hz, 1H), 4.31 (dd, J = 10.9, 3.1 Hz, 1H), 4.06 (dd, J = 10.9, 5.7 Hz, 1H), 3.42 (bs, 1H), 2.94 (t, J = 4.6 Hz, 1H), 2.86-2.76 (m, 1H). LCMS: Method 1: RT: 0.60 min; M+H<sup>+</sup>: 240.02.

**Synthesis of 1-(9H-carbazol-2-yloxy)-3-[2-(2-methoxyphenoxy)ethylamino]propan-2-ol (21).**

A mixture of **20** (0.13 g, 0.56 mmol) and 2-(2-methoxyphenoxy)ethanamine (0.095 g, 0.56 mmol) in ethanol (15 mL) was stirred at 65 °C for 16 h. The solvent was removed under reduced pressure and the residue was purified by flash column chromatography gradient elution of DCM/methanol (100/0 to 95/5). The compound obtained was further purified by flash column chromatography gradient elution of DCM/methanol = (100/0 to 90/20) to give **21** as a colourless solid (0.076 g, 33%). <sup>1</sup>H NMR (DMSO 600 MHz): δ 11.08 (s, 1H), 7.96 (d, J = 7.7 Hz, 1H), 7.93 (d, J = 8.5 Hz, 1H), 7.40 (d, J = 8.0 Hz, 1H), 7.29-7.23 (m, 1H), 7.11-7.06 (m, 1H), 6.97-6.92 (m, 3H), 6.89-6.82 (m, 2H), 6.76 (dd, J = 8.5, 2.2 Hz, 1H), 5.14-5.03 (m, 1H), 4.03-3.98 (m, 3H), 3.97-3.95 (m, 2H), 3.72 (s, 3H), 2.90 (t, J = 5.6 Hz, 2H), 2.79 (dd, J = 11.9, 3.9 Hz, 1H), 2.69 (dd, J = 11.8, 6.4 Hz, 1H); <sup>13</sup>C NMR (DMSO 151 MHz): δ 158.31, 149.59, 148.50, 141.48, 140.16, 124.56, 123.09, 121.47, 121.32, 121.16, 119.69, 118.96, 116.62, 114.01, 112.61, 111.04, 108.55, 95.63, 71.39, 68.77, 55.89, 52.93, 48.94; LCMS: Method 3, RT = 12.59; M+H<sup>+</sup>: 407.15.

**Synthesis of 9-(oxiran-2-ylmethyl)carbazole (22).** KOH (0.20 g, 3.59 mmol) was added to a solution of 9H-carbazole (0.50 g, 2.99 mmol) in acetonitrile (5 mL) and the reaction mixture was stirred at room temperature 1 h. Then, the reaction mixture was cooled in an icebath and 2-(bromomethyl)oxirane (0.64 mL, 7.48 mmol) was added dropwise. After the addition, the ice bath was removed and the reaction mixture was stirred at room temperature for 20 h. After this period, the reaction mixture was partitioned between ethyl acetate and water, and the organic layer was washed with water and brine, dried over MgSO<sub>4</sub>, filtered and concentrated. The residue was triturated with hexane, and recrystallized from ethyl acetate/ hexanes to yield **22** as a colourless solid (0.48 g, 68%) and used in the next step with no further purification. <sup>1</sup>H NMR (CDCl<sub>3</sub> 500 MHz): δ 8.11 (dt, J = 7.8, 1.0 Hz, 2H), 7.53-7.45 (m, 4H), 7.31-7.24 (m, 2H), 7.27

1 (s, 2H), 4.64 (dd, J = 15.9, 3.4 Hz, 1H), 4.42 (dd, J = 15.9, 4.8 Hz, 1H), 3.38-3.35 (m, 1H), 2.82  
(t, J = 4.4 Hz, 1H), 2.59 (dd, J = 4.8, 2.5 Hz, 1H); LCMS: Method 2, RT = 3.03 min; M+H<sup>+</sup>:  
224.15.

**Synthesis of 1-carbazol-9-yl-3-(2-phenylethylamino)propan-2-ol (23).** A solution of **22** (0.10 g, 0.43 mmol) and phenethylamine (0.05 mL, 0.43 mmol) in ethanol (5 mL) was stirred at 65 °C for 16 h. Then, the solvent was removed under reduced pressure and the residue was purified by flash column chromatography gradient elution of petroleum ether/ethyl acetate = (100/0 to 0/100) to give **23** as a colourless oil (0.07 g, 49%). <sup>1</sup>H NMR (DMSO 600 MHz): δ 8.11 (d, J = 7.6 Hz, 2H), 7.57 (d, J = 8.2 Hz, 2H), 7.40 (t, J = 7.6 Hz, 2H), 7.26 (t, J = 7.5 Hz, 2H), 7.20 (d, J = 7.5 Hz, 2H), 7.16 (t, J = 7.4 Hz, 3H), 5.02 (s, 1H), 4.43 (dd, J = 14.8, 5.3 Hz, 1H), 4.24 (dd, J = 14.8, 6.7 Hz, 1H), 3.97 (p, J = 5.9 Hz, 1H), 2.77-2.66 (m, 4H), 2.60 (dd, J = 11.8, 4.9 Hz, 1H), 2.54 (dd, J = 11.8, 6.1 Hz, 1H). <sup>13</sup>C NMR (DMSO 151 MHz): δ 141.03, 140.92, 129.07, 128.67, 126.27, 125.93, 122.45, 120.47, 119.05, 110.17, 69.24, 53.46, 51.66, 47.48, 36.47. LCMS: Method 3, RT = 12.76 min; M+H<sup>+</sup>: 345.15.

**Synthesis of N-[2-(2-methoxyphenoxy)ethyl]-2-morpholino-ethanamine (24).** A mixture of 4-(2-aminoethyl)morpholine (0.28 mL, 2.16 mmol), **3** (0.50 g, 2.16 mmol) and TEA (0.90 mL, 6.49 mmol) in THF (25 mL) was stirred at 65 °C for 4 h. After this time, the solvent was removed under reduced pressure and the residue was purified by reverse phase chromatography gradient elution of water/methanol = 90/10 to 0/100 to give **24** as a colourless oil (0.055 g, 9%). <sup>1</sup>H NMR (DMSO 500 MHz): δ 7.03-6.90 (m, 2H), 6.88-6.82 (m, 2H), 3.96 (t, J = 5.6 Hz, 2H), 3.72 (s, 4H), 3.52 (t, J = 4.6 Hz, 4H), 2.83 (t, J = 5.5 Hz, 2H), 2.63 (t, J = 6.4 Hz, 2H), 2.36-2.29 (m, 6H). LCMS: Method 1: RT: 0.39 min; M+H<sup>+</sup>: 281.13.

# **Synthesis of 1-(9H-carbazol-4-yloxy)-3-[2-(2-methoxyphenoxy)ethyl-(2-**

**morpholinoethyl)amino]propan-2-ol (25).** A mixture of **24** (36.6 mg, 0.13 mmol) and **5** (30.6

mg, 0.13 mmol) in ethanol (15 mL) was stirred at 65 °C for 16 h. Then, the solvent was removed

under reduced pressure and the residue was purified by flash column chromatography gradient

elution of petroleum ether/ethyl acetate = (100/0 to 0/100) to give **25** as a colourless oil (0.022 g,

29%). <sup>1</sup>H NMR (CDCl<sub>3</sub> 500 MHz): δ 8.28 (d, J = 7.7 Hz, 1H), 8.17 (s, 1H), 7.41-7.32 (m, 2H),

7.30 (t, J = 8.0 Hz, 1H), 7.18-7.15 (m, 1H), 7.02 (d, J = 8.0 Hz, 1H), 6.94-6.75 (m, 4H), 6.68 (d,

J = 8.0 Hz, 1H), 4.35-4.28 (m, 1H), 4.23-4.18 (m, 2H), 4.09 (t, J = 5.6 Hz, 2H), 3.82 (s, 3H), 3.69

(t, J = 4.7 Hz, 4H), 3.18-3.03 (m, 3H), 3.00-2.91 (m, 2H), 2.89-2.79 (m, 1H), 2.67-2.39 (m, 6H).

<sup>13</sup>C NMR (CDCl<sub>3</sub> 126 MHz): δ 155.28, 149.38, 148.11, 140.89, 138.70, 126.71, 124.86, 122.89,

122.62, 121.24, 120.83, 119.46, 113.13, 112.64, 111.69, 110.00, 103.58, 101.17, 69.56, 68.68,

67.40, 66.63, 57.56, 56.60, 55.73, 55.63, 53.20, 51.72. LCMS: Method 3, RT = 12.76; M+H<sup>+</sup>:

520.30.

## **Biology**

### **Animal husbandry**

Tissues obtained from wildtype CD-1 mice (Charles Rivers, UK) of either sex, at postnatal day 2

(P2), were used for the preparation of the mouse cochlear cultures that were then used for

screening, live imaging with GTTR and electrophysiology. Animals were raised according to

Home Office guidelines, and all experiments were performed in accordance with the Home

Office Animals (Scientific Procedures) Act 1986 and with approval of the Animal Welfare and

Ethical Review Board at the University of Sussex.

## 1     **Mouse cochlear culture preparation**

2     Cochlear cultures were prepared from CD-1 mice as previously described by Russell and  
3     Richardson.<sup>28</sup> In brief, P2 pups were killed by cervical dislocation and surface sterilised by three  
4     one minute washes in 80% ethanol. Subsequent dissections were performed in Hanks Buffered  
5     Salt Solution (HBSS; Thermo Shandon 14025050) buffered with 10mM Hepes (Sigma H0887)  
6     (HBHBSS). Cochleae were removed from the bony labyrinth and explanted onto collagen-coated  
7     (Corning 354236) coverslips and immersed in rat cochlear culture media (RCM - 93% DMEM-  
8     F12, 7% fetal bovine serum and 10 µg ml<sup>-1</sup> ampicillin), sealed in Maximow slide assemblies and  
9     left to adhere to the collagen for 24 h at 37°C.

## 10    **Mouse cochlear culture protection assay**

11    Following 24 h incubation coverslips with adherent cochleae were removed from the Maximow  
12    slide assemblies, placed in 35 mm petri dishes (Greiner Bio-One 627161) and incubated for 48 h  
13    at 37°C in a 5% CO<sub>2</sub> incubator in the presence of 1 ml RCM:DMEM-F12 (1:4) containing either  
14    vehicle (0.5% DMSO), 5 µM gentamicin (Sigma G3632), 5 µM gentamicin along with selected  
15    concentrations of the potentially protective compounds, or the potential protectants alone.  
16    Initially a dose response experiment was run for the parent compound from which subsequent  
17    concentrations were selected. Following 48 h incubation, cultures were washed twice in  
18    phosphate buffered saline (PBS), fixed in 3.7% formaldehyde (Sigma F1635) and stained with  
19    TRITC-phalloidin (Sigma P1951). Cultures were mounted on glass slides with Vectashield  
20    (Vector Laboratories H-1000) and imaged using a Zeiss Axioplan microscope, captured with a  
21    40x objective (0.75 NA). Each screen was repeated 2 to 8 times.

## 22    **Confocal Imaging**

1 Confocal microscopy was used for high resolution imaging of the mechanosensory hair bundles  
2 in order to assess any morphological disruption induced by the compounds of interest.

3 Slides were imaged on a Leica SP8 confocal microscope, using the 561 nm laser (at 3%  
4 intensity) and a 100x 1.44 NA oil-immersion lens. Images were captured at a resolution of  
5 736x400 pixels (and a zoom of x 2.0 with a x4 line average), using a low detector gain (511) in  
6 order to reduce noise and improve image quality. Z-projections were created in ImageJ.

### 7 **Quantification of OHC survival**

8 For quantification of HC survival, images from the mid-basal region were analysed. Numbers of  
9 OHCs in a 300  $\mu$ m long segment of the cochlea were counted, at a position approximately 20%  
10 along the length of the cochlea from the basal end. The presence of a hair bundle was the  
11 criterion used as a marker of HC survival. Although HCs can survive without a bundle<sup>23, 29</sup> the  
12 latter is essential for sound transduction, and provides a viable marker when searching for an  
13 otoprotectant. IHCs were not counted, due to the lack of damage to this cell type caused by  
14 exposure to 5  $\mu$ M gentamicin.

### 15 **Electrophysiology on mouse cochlear cultures**

16 MET currents were recorded and analysed using previously described methods.<sup>20</sup> In brief, OHCs  
17 in organotypic cultures prepared from P2 CD-1 mice were studied, with recordings performed in  
18 cultures that had been maintained for 1–2 days *in vitro*. MET currents were recorded using the  
19 whole-cell configuration of the patch clamp technique both before and during compound  
20 exposure at membrane potentials ranging from -164 mV to +96 mV. Currents were elicited by  
21 stimulating the OHC hair bundles using a fluid jet from a pipette (tip diameter 8–10  $\mu$ m) driven  
22 by a piezoelectric disc.<sup>7, 30</sup> Mechanical stimuli (filtered at 1.0 kHz, 8-pole Bessel) were applied

as 45 Hz sinusoids with driver voltage amplitudes of  $\pm 40$  V. Currents were acquired using pClamp (Molecular Devices) software and stored on computer for off-line analysis. For all recordings series resistance compensation was applied (60-80%) and the average residual series resistance was calculated to be  $1.37 \pm 0.08$  M $\Omega$  (n=47). The average maximum MET current size was  $1.50 \pm 0.07$  nA (n=49), resulting in a maximum voltage drop across the residual series resistance of 2.1 mV, a value sufficiently small to not require any correction to quoted voltage values.

Dose response curves were fitted with the equation:

$$\frac{I}{I_c} = \frac{1}{1 + \left(\frac{[B]}{K_D}\right)^{n_H}} \quad (1)$$

where  $I_c$  is the control current in the absence of the compound,  $[B]$  is the concentration of the blocking compound,  $K_D$  is the half-blocking concentration and  $n_H$  is the Hill coefficient.

Permeation and block of the MET channel for carvedilol and **13** were quantified by fitting a two-barrier one binding-site model to the fractional block curves, as described in detail before.<sup>20, 31</sup> This model is similar to that used to describe block of the MET currents by DHS,<sup>7</sup> but modified to allow for Hill coefficients different from one.

### Block of GTTR loading into mouse cochlear culture hair cells

Coverslips were removed from the Maximow slide assemblies, placed in a Perspex viewing chamber and immersed in 500  $\mu$ L HBHBSS. Cultures were treated with either 100  $\mu$ M carvedilol, 100  $\mu$ M of the carvedilol derivative **13** or 1% DMSO as a control, with carvedilol and **13** being dissolved in this solvent. After 5 minutes incubation time at room temperature, GTTR

was added at a final concentration of 0.2  $\mu$ M and incubation was continued for a further 10 minutes. The culture was washed three times with HBHBSS, before live imaging on a Zeiss Axioplan2 microscope. A 60X water immersion lens was used to take images of both the apical and basal regions of the cochlea across a time range from 14 to 24 minutes post-GTTR application. Three repeats were conducted. For quantification, analysis was performed on images from the mid-basal region, 24 minutes post-GTTR application. Ten cells from the first row of OHCs central to the 1200 pixel image were analysed, as shown by the asterisk in Figure 16, obtaining intensity values from a 40x40 pixel region of interest (ROI). Three background ROIs were measured, averaged and subtracted from each individual cell value, which were then averaged and repeated across three trials. One background ROI was taken from non-sensory HC cellular space to account for any endocytic loading.

## Statistics

All graphical representations display mean  $\pm$  SEM. Numbers above bars denote the number of independent experimental replicates. One-way ANOVA was applied followed by Tukey's multiple comparisons test, assuming normal distribution of the data. For GTTR live imaging experiments, an unpaired t-test was used. Significance was set at  $* = p < 0.05$ ,  $** = p < 0.01$ ,  $*** = p < 0.001$ .

## Associated Content

## Supporting Information

The Supporting Information is available free of charge on the ACS Publications website. Molecular formula strings (CSV) are available.



1  
2  
3  
4  
5  
6  
7  
8  
9  
10  
11  
12  
13  
14  
15  
16  
17  
18  
19  
20  
21  
22  
23  
24  
25  
26  
27  
28  
29  
30  
31  
32  
33  
34  
35  
36  
37  
38  
39  
40  
41  
42  
43  
44  
45  
46  
47  
48  
49  
50  
51  
52  
53  
54  
55  
56  
57  
58  
59  
60

**1 Corresponding Author Information**

**2 Marco Derudas,** \* Email: [m.derudas@sussex.ac.uk](mailto:m.derudas@sussex.ac.uk); Phone +44(0)1273876591

**3 Author contributions:** <sup>¶</sup> These authors contributed equally to the work in this manuscript

**5 Acknowledgment**

**6** This work was supported by the Medical Research Council (MR/K005561/1 to CJK, GPR, and  
**7** SEW). All data are provided in the Results and the Experimental Section of the paper and in the  
**8** Supporting Information.

**9 Abbreviations Used**

**10** MET, mechano-electrical transducer; AG, aminoglycoside; ROS, reactive oxygen species; OHC,  
**11** outer hair cells; IHC, inner hair cell; DMF, dimethylformamide; TEA, triethylamine; HOBt, 1-  
**12** hydroxybenzotriazole; EDC, N-(3-Dimethylaminopropyl)-N'-ethylcarbodiimide; DIPEA, N,N-  
**13** diisopropylethylamine; GTTR, gentamicin Texas red; SAR, structure activity relationship; DHS,  
**14** dihydrostreptomycin; THF, tetrahydrofuran; DMC, dichloromethane.

**16 Keywords:** aminoglycosides, carvedilol, hearing loss, ototoxicity, otoprotection,  
**17** mechanotransduction

**18 References**

**19** (1) Avent, M. L.; Rogers, B. A.; Cheng, A. C.; Paterson, D. L. Current use of  
**20** aminoglycosides: indications, pharmacokinetics and monitoring for toxicity. *Intern. Med.*

- 1  
2  
3 1 *J.* **2011**, *41*, 441-449.
- 4  
5 2 (2) Prayle, A.; Smyth, A. R. Aminoglycoside use in cystic fibrosis: therapeutic strategies and  
6  
7 toxicity. *Curr. Opin. Pulm. Med.* **2010**, *16*, 604-610.
- 8  
9  
10 3  
11 4 (3) Horsburgh, C. R. Jr; Barry, C. E. III; Lange, C. Treatment of tuberculosis. *N. Engl. J.*  
12  
13 *Med.* **2015**, *373*, 2149-2160.
- 14  
15  
16 5  
17 6 (4) Rizzi, M. D.; Hirose, K. Aminoglycoside ototoxicity. *Curr. Opin. Otolaryngol. Head*  
18  
19 *Neck Surg.* **2007**, *15*, 352-357. doi:10.1097/MOO.0b013e3282ef772d
- 20  
21 7  
22 8 (5) Hashino, E.; Shero, M. Endocytosis of aminoglycoside antibiotics in sensory hair cells.  
23  
24 *Brain Res.* **1995**, *704*, 135-140. doi:10.1016/0006-8993(95)01198-6
- 25  
26 9  
27 10 (6) Gale, J. E.; Marcotti, W.; Kennedy, H. J.; Kros, C. J.; Richardson, G. P. FM1-43 dye  
28  
29 behaves as a permeant blocker of the hair-cell mechanotransducer channel. *J. Neurosci.*  
30  
31 **2001**, *21*, 7013-7025. DOI: <https://doi.org/10.1523/JNEUROSCI.21-18-07013.2001>
- 32  
33 12  
34 13 (7) Marcotti, W.; Van Netten, S. M.; Kros, C. J. The aminoglycoside antibiotic  
35  
36 dihydrostreptomycin rapidly enters mouse outer hair cells through the mechano-electrical  
37  
38 transducer channels: aminoglycoside entry into hair cells. *J. Physiol.* **2005**, *567*, 505-521.  
39  
40 doi:10.1113/jphysiol.2005.085951
- 41  
42 14  
43 15 (8) Wang, Q.; Steyger, P. S. Trafficking of systemic fluorescent gentamicin into the cochlea  
44  
45 and hair cells. *J. Assoc. Res. Otolaryngol.* **2009**, *10*, 205-219. doi:10.1007/s10162-009-  
46  
47 0160-4
- 48  
49 16  
50 17 (9) Alharazneh, A.; Luk, L.; Huth, M.; Monfared, A.; Steyger, P. S.; Cheng, A. G.; Ricci, A.  
51  
52 J. Functional hair cell mechanotransducer channels are required for aminoglycoside  
53  
54 ototoxicity. *PLoS ONE* **2011**, *6*, e22347. doi:10.1371/journal.pone.0022347
- 55  
56 18  
57 19 (10) Owens, K. N.; Coffin, A. B.; Hong, L. S.; Bennett, K. O.; Rubel, E. W.; Raible, D. W.

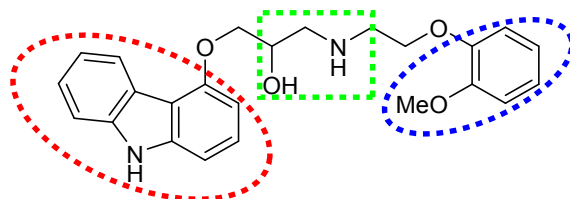
- 1  
2  
3 1 Response of mechanosensory hair cells of the zebrafish lateral line to aminoglycosides  
4  
5 2 reveals distinct cell death pathways. *Hear. Res.* **2009**, *253*, 32–41.  
6  
7 doi:10.1016/j.heares.2009.03.001  
8  
9  
10 4 (11) Coffin, A. B.; Rubel, E. W.; Raible, D. W. Bax, Bcl2, and p53 differentially regulate  
11  
12 neomycin- and gentamicin-induced hair cell death in the zebrafish lateral line. *J. Assoc.*  
13  
14 *Res. Otolaryngol.* **2013**, *14*, 645–659. doi:10.1007/s10162-013-0404-1  
15  
16  
17 7 (12) Coffin, A. B.; Williamson, K. L.; Mamiya, A.; Raible, D. W.; Rubel, E. W. Profiling  
18  
19 drug-induced cell death pathways in the zebrafish lateral line. *Apoptosis* **2013**, *18*, 393–  
20  
21 408. doi:10.1007/s10495-013-0816-8  
22  
23  
24 10 (13) Jiang, M.; Karasawa, T.; Steyger, P. S. Aminoglycoside-induced cochleotoxicity: a  
25  
26 11 review. *Front. Cell. Neurosci.* **2017**, *11*, 308. doi.org/10.3389/fncel.2017.00308  
27  
28  
29 12 (14) O’Sullivan, M. E.; Perez, A.; Lin, R.; Sajjadi, A.; Ricci, A. J.; Cheng, A. G. Towards the  
30  
31 13 prevention of aminoglycoside-related hearing loss. *Front. Cell. Neurosci.* **2017**, *11*, 325.  
32  
33 14 doi.org/10.3389/fncel.2017.00325  
34  
35  
36 15 (15) Jensen-Smith, H. C.; Hallworth, R.; Nichols, M. G. Gentamicin rapidly inhibits  
37  
38 16 mitochondrial metabolism in high-frequency cochlear outer hair cells. *PLoS ONE* **2012**,  
39  
40 17 7, e38471. doi:10.1371/journal.pone.0038471  
41  
42  
43 18 (16) Huth, M.E.; Han, K.-H.; Sotoudeh, K.; Hsieh, Y.-J.; Effertz, T.; Vu, A. A.; Verhoeven,  
44  
45 19 S.; Hsieh, M. H.; Greenhouse, R.; Cheng, A. G.; Ricci, A. J. Designer aminoglycosides  
46  
47 20 prevent cochlear hair cell loss and hearing loss. *J. Clin. Invest.* **2015**, *125*, 583-592.  
48  
49 21 doi.org/10.1172/JCI77424.  
50  
51  
52 22 (17) Duscha, S.; Boukari, H.; Shcherbakov, D.; Salian, S.; Silva, S.; Kendall, A.; Kato, T.;  
53  
54 23 Akbergenov, R.; Perez-Fernandez, D.; Bernet, B.; Vaddi, S.; Thommes, P.; Schacht, J.;  
55  
56  
57  
58  
59  
60

- 1  
2  
3 1 Crich, D.; Vasella, A.; Böttger, E. C. Identification and evaluation of improved 4'-O-  
4  
5 2 (alkyl) 4,5-disubstituted 2-deoxystreptamines as next-generation aminoglycoside  
6  
7 antibiotics. *MBio* **2014**, *5*, e01827-14. doi: 10.1128/mBio.01827-14, 1-10.  
8 3  
9  
10 4 (18) Avent, M. L.; Rogers, B. A.; Cheng, A. C.; Paterson, D. L. Current use of  
11  
12 aminoglycosides: indications, pharmacokinetics and monitoring for toxicity:  
13 5  
14 aminoglycosides: review and monitoring. *Intern. Med. J.* **2011**, *41*, 441–449.  
15 6  
16 doi:10.1111/j.1445-5994.2011.02452.x  
17 7  
18  
19 8 (19) Kamogashira, T.; Fujimoto, C.; Yamasoba, T. Reactive oxygen species, apoptosis, and  
20  
21 mitochondrial dysfunction in hearing loss. *BioMed. Res. Int.* **2015**, *2015*, 617207, 1-7.  
22 9  
23 doi:10.1155/2015/617207  
24 10  
25  
26 11 (20) Kirkwood, N. K.; O'Reilly, M.; Derudas, M.; Huckvale, R.; Kenyon, E. J.; Ward, S.E.;  
27  
28 Richardson, G. P.; Kros C. J. d-Tubocurarine and berbamine: alkaloids that are permeant  
29 12  
30 blockers of the hair cell's mechano-electrical transducer channel and protect from  
31 13  
32 aminoglycoside toxicity. *Front. Cell. Neurosci.* **2017**, *11*, 262, 1-15.  
33 14  
34 doi.org/10.3389/fncel.2017.00262  
35 15  
36  
37 16 (21) Kenyon, E. J.; Kirkwood, N. K.; Kitcher, S. R.; O'Reilly, M.; Derudas, M.; Cantillon, D.  
38  
39 M.; Goodyear, R. J.; Secker, A.; Baxendale, S.; Bull, J. C.; Waddell, S. J.; Whitfield, T.  
40 17  
41 T.; Ward, S. E.; Kros C. J.; Richardson, G. P. Identification of ion-channel  
42 18  
43 agonists/antagonists that protect against aminoglycoside-induced hair-cell death. *J. Clin.*  
44 19  
45 *Invest. Insight* **2017**, *2*, e96773. 10.1172/jci.insight.96773  
46 20  
47  
48  
49 21 (22) Ou, H. C.; Cunningham, L. L.; Francis, S. P.; Brandon, C. S.; Simon, J. A.; Raible, D.  
50  
51 W.; Rubel, E. W. Identification of FDA-approved drugs and bioactives that protect hair  
52 22  
53 cells in the zebrafish (*danio rerio*) lateral line and mouse (*mus musculus*) utricle. *J.*  
54 23  
55  
56  
57  
58  
59  
60

- 1  
2  
3 1 *Assoc. Res. Otolaryngol.* **2009**, *10*, 191–203. doi:10.1007/s10162-009-0158-y
- 4  
5 2 (23) Majumder, P.; Moore, P. A.; Richardson, G. P.; Gale, J. E. Protecting mammalian hair  
6  
7 cells from aminoglycoside-toxicity: assessing phenoxybenzamine's potential. *Front. Cell.*  
8  
9 *Neurosci.* **2017**, *11*, 94, 1-11. doi:10.3389/fncel.2017.00094
- 10  
11 4  
12 5 (24) Chowdhury, S.; Owens, K. N.; Herr, R. J.; Jiang, Q.; Chen, X.; Johnson, G.; Groppi, V.  
13  
14 E.; Raible, D. W.; Rubel, E. W.; Simon, J. A. Phenotypic optimization of urea–thiophene  
15  
16 carboxamides to yield potent, well tolerated, and orally active protective agents against  
17  
18 aminoglycoside-induced hearing loss. *J. Med. Chem.* **2018**, *61*, 84-97.  
19  
20 8  
21 9 10.1021/acs.jmedchem.7b00932
- 22  
23 10 (25) Tran Ba Huy, P.; Manuel, C.; Meulemans, A.; Sterkers, O.; Amiel, C. Pharmacokinetics  
24  
25 of gentamicin in perilymph and endolymph of the rat as determined by  
26  
27 radioimmunoassay. *J. Infect. Dis.* **1981**, *143*, 476-486.
- 28  
29 12  
30 13 (26) Wyman, J.; Gill, S. J. Binding and Linkage: Functional Chemistry of Biological  
31  
32 Macromolecules. University Science Books; Mill Valley, CA. 1990.
- 33  
34 14  
35 15 (27) Steyger, P. S.; Peters, S. L.; Rehling, J.; Hordichok, A.; Dai, C. F. Uptake of gentamicin  
36  
37 by bullfrog saccular hair cells in vitro. *J. Assoc. Res. Otolaryngol.* **2003**, *4*, 565–578.  
38  
39 16  
40 17 doi:10.1007/s10162-003-4002-5
- 41  
42 18 (28) Russell, I. J.; Richardson G. P. The morphology and physiology of hair cells in  
43  
44 organotypic cultures of the mouse cochlea. *Hear. Res.* **1987**, *31*, 9-24. doi: 10.1016/0378-  
45  
46 5955(87)90210-3
- 47  
48 20  
49 21 (29) Gale, J. E.; Meyers, J. R.; Periasamy, A.; Corwin, T. Survival of bundleless hair cells and  
50  
51 subsequent bundle replacement in the bullfrog's saccule. *J. Neurobiol.* **2002**, *50*, 81–92.  
52  
53 22  
54 23 doi:10.1002/neu.10002
- 55  
56  
57  
58  
59  
60

- (30) Kros, C.J.; Rüsch, A.; Richardson, G. P. Mechano-electrical transducer currents in hair cells of the cultured neonatal mouse cochlea. *Proc. Biol. Sci.* **1992**, *249*, 185-193. doi: 10.1098/rspb.1992.0102
- (31) van Netten, S. M.; Kros, C. J. Insights into the pore of the hair cell transducer channel from experiments with permeant blockers. *Curr. Top. Membr.* **2007**, *59*, 375-398. doi: 10.1016/S1063-5823(06)59013-1

### TOC Graphic



**SAR of Carvedilol**  
**From adrenergic blocker to otoprotectant against**  
**aminoglycoside-induced damage**